An extended thermodynamic model for size-dependent thermoelectric properties at nanometric scales: application to nanofilms, nanocomposites and thin nanocomposite films

H. Machrafi*
Université de Liège, Thermodynamique des Phénomènes Irréversibles, Allée du 6-Août, 17, BE-4000 Liège, Belgium
*H.Machrafi@ulg.ac.be

Abstract
A new mathematical model is developed, describing size-dependent subcontinuum thermoelectric properties from an extended thermodynamic point of view. This model takes into account the non-local effects of heat transfer through phonons and electrons that are important at nanometric scales. These phenomena are extended to apply also for electric transfer as well as the Seebeck coefficient. This model includes at nanoscale size-dependent electron and phonon thermal conductivities, electric conductivity, Seebeck coefficient and carrier concentrations. We compared nanofilms to nanocomposites and assessed their thermoelectric performances in the form of a figure of merit using as an example Bismuth and BismuthTelluride materials. It appeared that the figure of merit increases considerably for nanofilms and nanocomposites with respect to bulk materials. This is caused by the scattering of phonons and electrons. Our model shows that this scattering effect is not only present at the boundary or particle-matrix interface of the nanosized material, but also within it. The effect of particle size and surface specularity has been investigated, showing that a decreasing value of the particle size and specularity increases the scattering effect and improves the thermoelectric properties. An extension towards thin films of nanocomposite has been presented.

Key words: extended irreversible thermodynamics, thermoelectric properties, figure of merit, phonon and electron scattering, nanometric scale

1. Introduction

Transport properties play a central role in materials sciences. One of the current interests lies in the optimal application of thermoelectricity to convert (waste) heat to usable electricity (the Seebeck effect) [1]. This requires materials with high Seebeck coefficient, high electrical conductivity and low thermal conductivity. This is not an easy task because usually a high electrical conductivity implies also a high thermal conductivity, the two being linked as seen later in this paper. Other effects include the Peltier effect, where it is an electricity current that heats the material, and the Thomson effect, which is a combination of the former two [2]. Recently, research on thermoelectric materials has known an extraordinary burst [3]. A combination of the Seebeck coefficient, the electrical and thermal conductivities are found to be directly related to the efficiency of thermoelectric energy conversion. The combination of the aforementioned parameters is often resumed into a so-called figure of merit Z, or the dimensionless version $ZT = TS^2\sigma_e/(k_e + k_{ph})$, with T the temperature, S the Seebeck coefficient, σ_e the electric conductivity, k_e the electron thermal conductivity (the contribution of the electrons to the heat transfer) and k_{ph} the phonon thermal conductivity (the contribution of the phonons to the heat transfer) [4-6]. The figure of merit has increased by more than one order of magnitude since the end of the twentieth century. This was in particular achieved in superlattices in which one dimension is smaller than the mean free path of phonons but larger than that of electrons. Many aim at increasing further this figure of merit by the use of nanostructured materials [7]. Therefore, we investigate in this work particular properties of thermal and electric conduction at nanoscales and apply this to nanostructured materials. Such

materials know a huge variety of applications, such as heat conduction enhancement in polyesters [8] or energy storage systems [9], to mention a few. As far as goes nanostructured materials for thermoelectric systems [10-13], a decrease in the thermal conductivity is often sought for in order to increase the figure of merit ZT [5,6,14]. The figure of merit is not only inversely dependent on the thermal conductivity, but also depends on the electric conductivity, which are both size-dependent [7]. The figure of merit also depends on other material related properties, such as the hole and electron mobility's and carrier concentrations [11,12].
Nanostructured materials can be used in different forms. We are interested here in nanofilms and nanocomposites. Nanofilms can be between two other bulk materials and nanocomposites are generally made out of a homogeneous matrix in which nanoparticles are dispersed. For nanofilms and particles with characteristic lengths of the same order of magnitude or smaller than the phonon and electron mean free paths, the Fourier theory, based on the classical approach of thermodynamics, is not able to predict the heat flux thermal interactions between the nanofilm or nanoparticle and the bulk material next to it. Therefore, we propose to investigate the problem of heat conduction in nanostructured thermoelectric materials by a more sophisticated thermodynamic formalism, namely Extended Irreversible Thermodynamics (EIT) [15,16]. In this approach, the heat flux is elevated to the status of independent variable at the same footing as the temperature. The total heat flux $\boldsymbol{q}$ is assumed to be the sum of a phonon contribution $\boldsymbol{q_{ph}}$ and an electric one $\boldsymbol{q_e}$ [7], which are due to the phonon and electron motion through the material:

$$\boldsymbol{q} = \boldsymbol{q_e} + \boldsymbol{q_{ph}}. \tag{1}$$

In the presence of an electric field and without local heat supply, the partial energy balances for the phonons and the electrons are

$$\frac{\partial u_{ph}}{\partial t} + \nabla \cdot \boldsymbol{q_{ph}} = 0, \tag{2a}$$
$$\frac{\partial u_e}{\partial t} + \nabla \cdot \boldsymbol{q_e} = \boldsymbol{E} \cdot \boldsymbol{I}, \tag{2b}$$

with u_{ph}, u_e, $\boldsymbol{E}$ and $\boldsymbol{I}$ are the phonon internal energy, electron internal energy, the electric field and the electric-current density. The total energy balance is then, in the absence of a magnetic field, given by

$$\frac{\partial u}{\partial t} + \nabla \cdot \boldsymbol{q} = \boldsymbol{E} \cdot \boldsymbol{I}, \tag{3}$$

with

$$u = u_{ph} + u_e, \tag{4}$$

which also implies $C = C_{ph} + C_e$, used later on, C being the specific (at constant volume) heat capacity. The continuity law for electric charge is

$$\frac{\partial \rho_e}{\partial t} + +\nabla \cdot \boldsymbol{I} = 0, \tag{5}$$

with ρ_e the density of electric charge. These equations give us now the evolution of u_{ph}, u_e and ρ_e, with the corresponding fluxes $\boldsymbol{q_{ph}}$, $\boldsymbol{q_e}$ and $\boldsymbol{I}$. The basic principles of EIT allow postulating

additional evolution equations for these fluxes (who are now considered as independent variables) as [15]

$$\tau_{ph}\frac{\partial \boldsymbol{q_{ph}}}{\partial t}+\boldsymbol{q_{ph}}=-k_{ph}\nabla T+\Lambda_{ph}^2(\nabla^2\boldsymbol{q_{ph}}+2\nabla\nabla\cdot\boldsymbol{q_{ph}}), \tag{6a}$$

$$\tau_{e}\frac{\partial \boldsymbol{q_{e}}}{\partial t}+\boldsymbol{q_{e}}=-(k_e+\mathrm{S}\Pi\sigma_e)\nabla T+\Lambda_{e}^2(\nabla^2\boldsymbol{q_{e}}+2\nabla\nabla\cdot\boldsymbol{q_{e}})+\Pi\sigma_e\boldsymbol{E}, \tag{6b}$$

$$\tau_{I}\frac{\partial \boldsymbol{I}}{\partial t}+\boldsymbol{I}=\sigma_e(\boldsymbol{E}-\mathrm{S}\nabla T)+\Lambda_{I}^2(\nabla^2\boldsymbol{I}+2\nabla\nabla\cdot\boldsymbol{I}), \tag{6c}$$

where τ, Λ and Π are the relaxation time, mean free path and the Peltier coefficient, respectively, the subscripts ph and e standing for phonon and electron, respectively. The last term in Eq. (6a) denotes the Guyer-Krumhansl contribution to denote the non-locality of the phonon heat flux, while the equivalents are also present in Eqs. (6b)-(6c) for the electron heat flux and electric-current density, respectively. When the Guyer-Krumhansl contribution is neglected, we obtain the Cattaneo equation [17] and if furthermore, the time-dependency is neglected, the classical Fourier law is obtained. Eq. (6b) is obtained with the hypothesis that the electronic heat flux is governed by the same principles as the phonon one in Eq. (6a) with additional terms for the Peltier effect in Eq. (6b). Neglecting again the Guyer-Krumhansl and time dependency terms in Eq. (6b) gives the classical equation describing the Peltier effect [7]. Since the electric current also passes through the same material, we assume also that it follows the same thermodynamic principles as Eq. (6a) and (6b). Neglecting Guyer-Krumhansl and the time dependency term in Eq. (6c) gives $\boldsymbol{I}=\sigma_e(\boldsymbol{E}-\mathrm{S}\nabla T)$ and omitting also an electrical field gives $\boldsymbol{I}=-\mathrm{S}\sigma_e\nabla T$, which shows that an electric current can be obtained by a temperature gradient, which is called the Seebeck effect. In the absence of an imposed electric field (where we do not consider the Peltier effect), Eq. (6) reduces to

$$\tau_{ph}\frac{\partial \boldsymbol{q_{ph}}}{\partial t}+\boldsymbol{q_{ph}}=-k_{ph}\nabla T+\Lambda_{ph}^2(\nabla^2\boldsymbol{q_{ph}}+2\nabla\nabla\cdot\boldsymbol{q_{ph}}), \tag{7a}$$

$$\tau_{e}\frac{\partial \boldsymbol{q_{e}}}{\partial t}+\boldsymbol{q_{e}}=-k_{e}\nabla T+\Lambda_{e}^2(\nabla^2\boldsymbol{q_{e}}+2\nabla\nabla\cdot\boldsymbol{q_{e}}), \tag{7b}$$

$$\tau_{I}\frac{\partial \boldsymbol{I}}{\partial t}+\boldsymbol{I}=-\mathrm{S}\sigma_e\nabla T+\Lambda_{I}^2(\nabla^2\boldsymbol{I}+2\nabla\nabla\cdot\boldsymbol{I}). \tag{7c}$$

This development suggests that in order to account for non-local effects, higher order fluxes should be taken into account. Also, it shows nicely the relation between on one side an imposed temperature gradient (for instance, the heat from sunrays) and on the other side a heat flux and electric current. The system (1)-(6) (of which (7) is a special case) can be applied to calculate the efficiency of thermoelectric systems [3]. This is, however, not the purpose of this work. Before calculating the efficiency of thermoelectric systems, it is important to investigate first the optimal conditions that allow such an efficiency to be improved. Such conditions are set by an optimization of the physical parameters that are present in the equations (1)-(6): the phonon and electron contributions of the thermal conductivity, the Seebeck coefficient and the electric conductivity. As will be of use later on, the system (1)-(6) shows also the analogy between these different physical parameters in that they all appear before the temperature gradient.
The way the heat flux and the electric current pass through the thermoelectric material is crucial for its performance and depends directly on the phonon thermal conductivity, electron thermal conductivity and electric conductivity as is shown in system (7). The figure of merit has for bulk materials a typical non-dimensional value around 1 and is a complex interaction between

the thermal conductivity, electric conductivity and the Seebeck coefficient, which depends on the carrier concentration. While it is already known that the figure of merit can be increased by using nanoscaled materials, it is the purpose of this paper to model quantitatively the phenomena of the several thermo-electric components of the figure of merit at nanoscale. In doing this, it is aimed to propose a concrete easy-to-use formulation that still captures the several nanoscale features that influence the figure of merit. Non-local effects of heat transfer by phonons and electrons become important at nanoscale and Fourier's law is no longer applicable. Cattaneo's adaptation of Fourier's law shows improvement for high frequency systems, but still is not accurate at nanoscale. Via a new thermodynamic formulation, taking into account the aforementioned non-local effects, we show that size-effects at nanoscale become important.
The theoretical principles of EIT are briefly discussed in section 2. The development for the thermoelectric properties is performed in section 3, with an application to nanofilms and nanocomposites. Section 4 presents a Gedankenexperiment extending the previous model to thin films of nanocomposites. In this work, we use Bismuth (Bi) and p-type BismuthTelluride (Bi_2Te_3) as an example, of which the material properties are presented in section 5. The results are discussed in section 6. Section 7 shows the results of the Gedankenexperiment, followed by the conclusion in section 8.

2. Theory of Extended Irreversible Thermodynamics for nanoscale heat and electric transfer

We will derive here the thermal conductivity valid at nanoscales. This is done using EIT, the use of which is elucidated in this subsection. We will perform this by deriving the phonon contribution of the thermal conductivity $k_{ph,\mathcal{N}}$ at nanoscales, with the subscript $\mathcal{N}$ designating the nanoscale. The electron contribution of the thermal conductivity $k_{e,\mathcal{N}}$ is exactly the same, by replacing the phonon specific heat C_{ph}, phonon lattice velocity v_{ph} and phonon mean free path $\Lambda_{ph,b}$ by the electron specific heat C_e, electron thermal velocity v_e and electron mean free path $\Lambda_{e,b}$, respectively. The analogy of the electron contribution with that of the phonon one is generally proposed throughout the paper. From a physical point of view, we can consider the phonons and the electrons as gas-like constituents that have both gas-like behavior, flowing through the material lattice. Since we consider that both the phonons and the electrons behave like a gas, we assume that they also follow the same thermodynamic principles. Therefore, the non-local effects that are introduced by EIT (in the framework of this paper) for the phonon contribution, apply also for the electron contribution of the thermal conductivity. As they also apply for the electron contribution, the electrical conductivity can be treated in the same way in the same framework. The Seebeck coefficient that relates a temperature gradient with an electric current can then also be treated that way, albeit not directly. Indeed, the systems (6) and (7) show nicely that the thermal and electric conductivities precede the temperature gradient, while the Seebeck coefficient only precedes the temperature gradient in the form of a product with the electric conductivity. In subsection 2.2, this model is applied to nanofilm thermoelectric systems, including the electric conductivity, Seebeck coefficient, power factor and figure of merit, all in the light of EIT.
The phonon thermal conductivity at nanoscale is given by

$$k_{ph,\mathcal{N}} = k_{ph}^0 \, f(Kn, s), \tag{8}$$

wherein k_{ph}^0 is the value of the phonon thermal conductivity for the bulk material at macro scale (k_e^0 being the equivalent for the electron contribution of the thermal conductivity) and given by the classical Boltzmann phonon expression

$$k_{ph}^0 = \frac{1}{3}(C_{ph} v_{ph} \Lambda_{ph,b})|_{T_{ref}}, \tag{9}$$

the quantity $f(Kn, s)$ being a correction factor, taking into account the dimension of the nanoparticles, their shape and their specularity. T_{ref} is the reference temperature, say the room temperature. Moreover, Kn is the Knudsen number defined as the ratio of the mean free path of the phonons inside the nanomaterial $\Lambda_{ph,b}$ (the subscript b stands for the bulk material), and the "specular" characteristic length ℓ_s:

$$Kn_{ph} = \Lambda_{ph,b}/\ell_s. \tag{10}$$

The specular characteristic length ℓ_s is defined by

$$\ell_s = \ell(1+s)/(1-s), \tag{11a}$$
$$\ell \equiv \delta_{\mathcal{N}} \quad \text{(nanofilm)}, \tag{11b}$$
$$\ell \equiv r_p \quad \text{(nanocomposite)}, \tag{11c}$$

with $\delta_{\mathcal{N}}$ the nanofilm thickness (used in this subsection) and r_p the radius of a nanoparticle embedded in a nanocomposite (used in the next subsection). In expression (11a), the symbol s ($0 \leq s \leq 1$) denotes the surface specularity on the nanoscale material, expressing the probability of specular scattering of phonons on the boundary (whether it be that of the nanofilm or the nanoparticle). For $s = 0$, the surface is called diffuse, meaning that the direction of phonons after impact is independent of the direction of the impacting phonons, in which case ℓ_s is simply ℓ. For $s \to 1$, we have a surface on which the impacting phonons influence the direction of the out coming phonons and the surface is said to be perfectly specular. Another interesting interpretation of $s \to 1$, which should be kept in mind, is that the dimension of the nanoscale material becomes macroscale, i.e. $\ell \gg \Lambda_{ph,b}$ or $Kn_{ph} \to 0$.

It should also be noticed that the contribution of the phonon collisions is present in the correction factor $f(Kn)$ as well. The latter will now be determined by using EIT.

In the problem of a rigid heat conductor, the only relevant conserved variable is the internal energy e (or the temperature T) whereas the energy flux (here the heat flux vector $\boldsymbol{q}$) is the non-conserved flux variable so that the space of state variables is $\boldsymbol{V} = (e, \boldsymbol{q})$. In more complex materials like in nanomaterials, fluxes of higher order should be introduced as shown later on. The corner stone of EIT is to assume the existence of an entropy function $\eta(\boldsymbol{V})$ [15,18], depending on the whole set $\boldsymbol{V}$ of variables: here $\eta = \eta(e, \boldsymbol{q})$, or in terms of time derivatives,

$$d_t \eta(e, \boldsymbol{q}) = \frac{\partial \eta}{\partial e} d_t e + \frac{\partial \eta}{\partial \boldsymbol{q}} . d_t \boldsymbol{q} \tag{12}$$

wherein e and η are measured per unit volume and a dot stands for the scalar product. The symbol d_t designates the time derivative which is indifferently the material or the partial time derivative as the system is, respectively, in motion or at rest. It is assumed that η is a concave function of the variables to guarantee stability of the equilibrium state and that it obeys a general time-evolution equation of the form

$$d_t \eta = -\nabla \cdot \boldsymbol{J}^s + \sigma^s \qquad (\sigma^s \geq 0), \tag{13}$$

whose rate of production per unit volume σ^s (in short, the entropy production) is positive definite to satisfy the second principle of thermodynamics, the quantity $\boldsymbol{J}^s$ is the entropy flux. Let us define the local non-equilibrium temperature by $T^{-1}(e) = \partial\eta/\partial e$ (fundamental thermodynamic relation at constant volume) and select the constitutive equation for $\partial\eta/\partial\boldsymbol{q}$ as given by $\partial\eta/\partial\boldsymbol{q} = -\alpha(T)\boldsymbol{q}$, where $\alpha(T)$ is a material coefficient depending generally on T; it is positive definite in order to meet the property that s is maximum at equilibrium, the minus sign in front of $\alpha(T)\boldsymbol{q}$ has been introduced for convenience. Under these conditions, expression (12), referred to as the Gibbs equation, can be written as

$$d_t\eta(e,\boldsymbol{q}) = T^{-1}d_t e - \alpha_1\boldsymbol{q}.d_t\boldsymbol{q}, \tag{14}$$

wherein α_1 a phenomenological coefficient identified later on. However, expression (14) does not account for non-local effects. These non-local effects are elegantly introduced in the framework of EIT by appealing to a hierarchy of fluxes $\boldsymbol{Q}^{(1)}$, $\boldsymbol{Q}^{(2)}$, ..., $\boldsymbol{Q}^{(n)}$ with $\boldsymbol{Q}^{(1)}$ identical to the heat flux vector $\boldsymbol{q}$, $\boldsymbol{Q}^{(2)}$ (a tensor of rank two) is the flux of $\boldsymbol{q}$, $\boldsymbol{Q}^{(3)}$ the flux of $\boldsymbol{Q}^{(2)}$ and so on. From the kinetic theory point of view, the quantities $\boldsymbol{Q}^{(2)}$and $\boldsymbol{Q}^{(3)}$ represent the higher moments of the velocity distribution. Indeed, it follows from the kinetic theory that the relaxation times of the higher order fluxes are not shorter than the collision time. Therefore, using only the first-order fluxes as independent variables is not satisfactory to describe high-frequency processes, because when the frequency becomes comparable to the inverse of the relaxation time of the first-order flux, all the higher-order fluxes will behave also like independent variables and must be incorporated in the formalism. Up to the nth-order flux, the Gibbs equation generalizing relation (12) becomes

$$d_t\eta\left(e,\boldsymbol{q},\boldsymbol{Q}^{(1)},\dots,\boldsymbol{Q}^{(n)}\right) = T^{-1}d_t e - \alpha_1\boldsymbol{q}\cdot d_t\boldsymbol{q} - \alpha_2\boldsymbol{Q}^{(2)}\otimes d_t\boldsymbol{Q}^{(2)} - \cdots - \alpha_N\boldsymbol{Q}^{(n)}\otimes d_t\boldsymbol{Q}^{(n)}, \tag{15}$$

wherein the symbol $\otimes$ denotes the inner product of the corresponding tensors. The second step is the formulation of the entropy flux $\boldsymbol{J}^s$. It is natural to expect that it is not simply given by the classical expression $T^{-1}\,\boldsymbol{q}$, but that it will depend on higher order fluxes, as

$$\boldsymbol{J}^s = T^{-1}\boldsymbol{q} + \beta_1\boldsymbol{Q}^{(2)}\cdot\boldsymbol{q} + \cdots + \beta_{n-1}\boldsymbol{Q}^{(n)}\otimes\boldsymbol{Q}^{(n-1)}, \tag{16}$$

The next step is the derivation of the rate of entropy production per unit volume σ^s which is defined by

$$\sigma^s = d_t\eta + \nabla\cdot\boldsymbol{J}^s \geq \boldsymbol{0}, \tag{17}$$

and is a positive definite quantity according to the second law of thermodynamics. After substituting in (17) the expressions of $d_t\eta$ and $\boldsymbol{J}^s$ from (15) and (16), respectively, and eliminating $d_t e$ via the energy conservation law for rigid heat conductors ($d_t e = -\nabla\cdot\boldsymbol{q}$), one obtains

$$\sigma^s = -\left(-\nabla T^{-1} + \alpha_1 d_t\boldsymbol{q} - \beta_1\nabla\cdot\boldsymbol{Q}^{(2)}\right)\cdot\boldsymbol{q} - \cdots - \sum_{n=2}^{N}\boldsymbol{Q}^{(n)}\otimes\left(\alpha_n d_t\boldsymbol{Q}^{(n)} - \beta_n\nabla\cdot\boldsymbol{Q}^{(n+1)} - \beta_{n-1}\nabla\boldsymbol{Q}^{(n-1)}\right) \geq \boldsymbol{0} \tag{18}$$

The expression for σ^s is a bilinear relationship in the flux $\boldsymbol{q}$ and the subsequent higher order of fluxes $\boldsymbol{Q}^{(n)}$. The quantity represented by the two terms between the parentheses is usually called

the thermodynamic force $\boldsymbol{X}$. The simplest way to guarantee the positiveness of the entropy production σ^s is to assume a linear flux-force relation of the form $\boldsymbol{Q}^{(n)} = L\boldsymbol{X}$ ($n = 1,2,3, ...$), where L is a phenomenological coefficient. As such, we obtain

$$\nabla T^{-1} - \alpha_1 \partial_t \boldsymbol{Q}^{(1)} + \beta_1 \nabla \cdot \boldsymbol{Q}^{(2)} = \mu_1 \boldsymbol{Q}^{(1)}, \tag{19a}$$

$$\beta_{n-1} \nabla \boldsymbol{Q}^{(n-1)} - \alpha_n \partial_t \boldsymbol{Q}^{(n)} + \beta_n \nabla \cdot \boldsymbol{Q}^{(n+1)} = \mu_n \boldsymbol{Q}^{(n)}, (n = 2,3, ...), \tag{19b}$$

compatible with positive entropy production. In (19), ∂_t stands for the time derivative, and α_i, β_i and μ_i are phenomenological coefficients related to the relaxation times, correlation lengths and transport coefficients, respectively. Equation (19a) reduces to the well-known law of Cattaneo [17] when the term $\nabla \cdot \boldsymbol{Q}^{(2)}$ is omitted. We now consider an infinite number of flux variables ($n \to \infty$) and apply the spatial Fourier transform

$$\widehat{\boldsymbol{q}}(\boldsymbol{k}, t) = \int_{-\infty}^{+\infty} \boldsymbol{q}(\boldsymbol{r}, t) e^{-i\boldsymbol{k}\cdot\boldsymbol{r}} \, d\boldsymbol{r} \tag{20}$$

to Eqs. (19), with $\widehat{\boldsymbol{q}}$ the Fourier transform of $\boldsymbol{q}$, $\boldsymbol{r}$ the spatial variable, t the time and $\boldsymbol{k}$ the wavenumber vector. This procedure results into obtaining the following time-evolution equation for the heat flux:

$$\bar{\tau}(\boldsymbol{k}) \partial_t \widehat{\boldsymbol{q}}(\boldsymbol{k}, t) + \widehat{\boldsymbol{q}}(\boldsymbol{k}, t) = -i\boldsymbol{k} k_{\mathcal{N},ph}(\boldsymbol{k}) \widehat{T}(\boldsymbol{k}, t) \tag{21}$$

where $\bar{\tau}(\boldsymbol{k}) = \alpha_1/\mu_1$ designates a renormalized relaxation time depending generally on $\boldsymbol{k}$. $k_{\mathcal{N},ph}(\boldsymbol{k})$ is given by the continued-fraction for the $\boldsymbol{k}$–dependent effective thermal conductivity:

$$k_{\mathcal{N},ph}(\boldsymbol{k}) = \cfrac{k_{ph}^0}{1+\cfrac{\boldsymbol{k}^2 l_1^2}{1+\cfrac{\boldsymbol{k}^2 l_2^2}{1+\cfrac{\boldsymbol{k}^2 l_3^2}{1+\cdots}}}}, \tag{22}$$

with k_{ph}^0 the classical bulk thermal conductivity, given by Eq. (9), independent of the dimension of the system, l_n is the correlation length of order n defined by $l_n^2 = \beta_n^2/(\mu_n \mu_{n+1})$. Here, it is assumed that the relaxation times τ_n ($n > 1$) corresponding to higher order fluxes are negligible with respect to τ_1, which is a hypothesis generally admitted in kinetic theories. In the present problem, there is only one dimension (either the nanofilm thickness or the nanoparticle radius), so that it is natural to define $k \equiv 2\pi/\ell_s$. The correlation lengths selected as $l_n^2 = a_{n+1} l^2$, with $a_n = n^2/(4n^2 - 1)$ and l identified as the mean free path independently of the order of approximation. This is a rather natural choice for phonons as shown by Dreyer and Struchtrup [19]. With these results in mind, the continued fraction (22) reduces to an asymptotic limit (see for mathematical formulation Ref. [20]), leading finally to the following expression for $k_{\mathcal{N},ph}$:

$$k_{ph,\mathcal{N}} = \frac{3k_{ph}^0}{4\pi^2 {Kn_{ph}}^2} \left[\frac{2\pi Kn_{ph}}{arctan(2\pi Kn_{ph})} - 1 \right], \tag{23}$$

with Kn_{ph} given by Eq. (10).

3. Calculation of the thermoelectric properties

3.1 Model for nanofilm thermoelectric devices

In this subsection, we continue with the model presented in section 2.1 in order to apply it to nanofilm thermoelectric systems. In analogy with Eq. (23), we obtain also the following expression for the electron contribution of the thermal conductivity at nanoscales

$$k_{e,\mathcal{N}} = \frac{3k_e^0}{4\pi^2 {Kn_e}^2}\left[\frac{2\pi Kn_e}{arctan(2\pi Kn_e)} - 1\right], \tag{24}$$

where $Kn_e = \Lambda_{e,b}/\ell_s$ in analogy with Eq. (10). The total thermal conductivity at nanoscales is then defined as

$$k_{tot,\mathcal{N}} = k_{ph,\mathcal{N}} + k_{e,\mathcal{N}}.$$

The electric conductivity at nanoscale is defined in analogy to the electron contribution of the thermal conductivity as

$$\sigma_{\mathcal{N}} = \frac{k_{e,\mathcal{N}}}{LT}, \tag{25}$$

or

$$\sigma_{\mathcal{N}} = \frac{3k_e^0}{4\pi^2 {Kn_e}^2 LT}\left[\frac{2\pi Kn_e}{arctan(2\pi Kn_e)} - 1\right], \tag{26}$$

with $k_e^0 \equiv \sigma^0 LT$, where L is the Lorentz number and T the absolute temperature. The Lorentz number is determined by

$$L = \frac{\pi^2}{3}\left(\frac{k_B}{e_c}\right)^2, \tag{27}$$

where k_B is Boltzmann's constant and e_c the elementary charge. Furthermore, the electric conductivity of a bulk material is not only dependent on the electron contribution of the thermal conductivity, but also on the electron n_n and hole n_p carrier concentration as well as electron μ_n and hole μ_p mobility [21]:

$$\sigma^0 = n_n e_c \mu_n + n_p e_c \mu_p. \tag{28}$$

Here, the subscripts n and p stand for the denomination of n-type and p-type carriers, typically used for electrons and holes, respectively. The thermoelectric performance is typically assessed by the figure of merit $Z_{\mathcal{N}}$, where the non-dimensional version $ZT_{\mathcal{N}}$ is given by

$$ZT_{\mathcal{N}} = T\frac{S_{\mathcal{N}}^2 \sigma_{\mathcal{N}}}{k_{ph,\mathcal{N}} + k_{e,\mathcal{N}}} = \frac{S_{\mathcal{N}}^2/L}{\frac{k_{ph,\mathcal{N}}}{k_{e,\mathcal{N}}} + 1}. \tag{29}$$

Here, $S_{\mathcal{N}}$ is the Seebeck coefficient (the electric conductivity in a material is determined via the mobility of both electrons and holes) given by [22]

$$S_{\mathcal{N}} = \frac{n_n \mu_n S_n + n_p \mu_p S_p}{n_n \mu_n + n_p \mu_p}. \tag{30}$$

with

$$S_x = (-1)^z \frac{8\pi^2 {k_B}^2}{3e_c h^2} m_x^* T \left(\frac{\pi}{3n_x}\right)^{2/3}, \tag{31}$$

where h is Planck's constant, m_x^* the effective mass of electrons or holes (expressed in free electron mass m^0) and the subscript x denoting whether it concerns the Seebeck coefficient of electrons ($x = n$ and $z = 1$) or that of holes ($x = p$ and $z = 2$). If the material is only of the n-type then $S_{\mathcal{N}} = S_n$ (< 0), while a p-type material would have $S_{\mathcal{N}} = S_p$ (> 0). With the Seebeck coefficient and the electric conductivity, a power factor can be defined as

$$PF_{\mathcal{N}} = S_{\mathcal{N}}^2 \sigma_{\mathcal{N}}. \tag{32}$$

There is still a note to be made. The carrier concentration of the holes and electrons cannot be assumed to stay constant with respect to the film's size. Nanoscaling causes the scattering of the carriers [23] (in the direction of the film thickness) at the film's boundary (ballistic effect). Since the carrier concentrations appear in the definition of the electric conductivity in Eq. (28), we assume that the variation of the carrier concentrations (and its scattering behavior) also follows that of the electric conductivity (which follows that of the thermal conductivity, described by EIT) at nanoscale (see Eq. (26)). Also, we should notice that the mobility will increase for decreasing carrier concentration, governed by an inverse power law [24]. From Eqs. (26) and (28) we have

$$n_x \mu_x \sim \sigma_{\mathcal{N}} = \frac{3\sigma^0}{4\pi^2 K {n_e}^2} \left[\frac{2\pi K n_e}{arctan(2\pi K n_e)} - 1\right], \tag{33}$$

Knowing that $S_x \sim n_x^{-2/3}$ from Eq. (31) and that $\sigma \sim n_x$ and noting that from [12] the power factor ${S_x}^2 \sigma \sim \mu_x$ (neglecting any variations of the effective mass), it can be easily deduced that $\mu_x \sim n_x^{-1/3}$ (also observed by [25]), which leads to:

$$n_x^{2/3} \sim \sigma_{\mathcal{N}}, \tag{34}$$

or

$$n_x = n_{x,0} \left(\frac{\sigma_{\mathcal{N}}}{\sigma^0}\right)^{3/2} = n_{x,0} \left(\frac{k_{e,\mathcal{N}}}{k_e^0}\right)^{3/2}, \tag{35}$$

with $n_{x,0}$ the carrier concentration of the bulk material (without taking into account the effect of electron scattering due to the nanoparticles). In this subsection, we have obtained a mathematical model for describing the thermal conductivity (with its phonon and electron contributions), the electric conductivity, the Seebeck coefficient (taking into account the scattering of the carriers and the change of the mobility) and the resulting figure of merit, all at nanoscale. This model is suitable for nanofilms and in section 4.1, we will apply this model as such. However, this model is also suitable for nanoparticles, with some modifications presented in section 2.2. Furthermore, since nanoparticles are embedded in a matrix (nanocomposites), the latter must also be taken into account. The next section will extend the present model for the use of nanocomposites.

3.2 Extension to nanocomposite thermoelectric devices

In this section, we use the models from section 2.1 and 2.2 in order to apply it for nanocomposites, making some modifications. Using the definition of the Knudsen number (10) and the corresponding equations (11), we can easily notice that (23) can, next to nanofilms, also be used for nanoparticles. The thermal conductivity (both phonon ($k_{ph,\mathcal{N}}$) and electron ($k_{e,\mathcal{N}}$) contributions) and electric conductivity ($\sigma_{\mathcal{N}}$) of the nanoparticles are then given keeping in mind that now $\ell \equiv r_p$. We will have to add the contribution of the bulk matrix ($k_{ph,m}$, $k_{e,m}$ and σ_m), respectively, within which the nanoparticles are embedded. As in the previous section, we will extend our model for the phonon contribution. The electron contribution follows exactly the same procedure, replacing the phonon specific heat $C_{ph,m}$, lattice velocity $v_{ph,m}$ and phonon mean free path $\Lambda_{ph,b,m}$ by the electron specific heat $C_{e,m}$, electron thermal velocity $v_{e,m}$ and electron mean free path $\Lambda_{e,b,m}$, respectively, m the subscript denoting that the property concerns the bulk matrix. The phonon thermal conductivity of the bulk matrix is given by the classical Boltzmann phonon expression:

$$k_{ph,m} = \frac{1}{3}\left(C_{ph,m} v_{ph,m} \Lambda_{ph,m}\right)|_{T_{ref}}. \tag{36}$$

Within the matrix, the phonons experience phonon-phonon interactions and the mean free path is given by the Matthiessen rule:

$$\frac{1}{\Lambda_{ph,m}} = \frac{1}{\Lambda_{ph,b,m}} + \frac{1}{\Lambda_{ph,coll,m}}. \tag{37}$$

with $\Lambda_{ph,b,m}$ designating the mean free path in the bulk matrix and $\Lambda_{coll,m}$ the supplementary contribution due to the interactions at the particle-matrix interface given by [26]

$$\Lambda_{coll,m} = \frac{4 r_{p,s}}{3\varphi}, \tag{38}$$

with φ the volume fraction of the nanoparticles in the matrix. This is a heterogeneous medium, which means that we cannot just use (23). We have said earlier that equation (23) can also be used for nanoparticles. Still, equation (23) is only valid for materials that are nanoscaled and homogeneous, the latter of which is obviously not the case for nanocomposites. Therefore, in order to calculate the thermal conductivity for nanocomposites, we have to relate the one in the nanoparticle (given by (23)) to the one in the bulk matrix (given by (36)). For this purpose, we will make use of the effective-medium approach [26-28] which provides a process of homogenization of the heterogeneous medium formed by the matrix and the particles. The effective medium theory calculates effective properties for media with located symmetric inclusions. The approach leads to exact formulas for the effective thermal conductivity [26-28]. The basic formula for the effective phonon thermal conductivity coefficient k_{ph}^{eff} is Maxwell's relation [29,30], which has been revisited by [26,27] and adapted here for our purposes

$$k_{ph}^{eff} = k_{ph,m} \frac{2k_{ph,m} + (1+2\alpha_{ph})k_{ph,\mathcal{N}} + 2\varphi[(1-\alpha_{ph})k_{ph,\mathcal{N}} - k_{ph,m}]}{2k_{ph,m} + (1+2\alpha_{ph})k_{ph,\mathcal{N}} - \varphi[(1-\alpha_{ph})k_{ph,\mathcal{N}} - k_{ph,m}]}. \tag{39}$$

In this expression, α is a dimensionless parameter describing the particle-matrix interaction:

$$\alpha_{ph} = R_{ph} k_{ph,m} / r_{p,s}. \tag{40}$$

The quantity R is the thermal boundary resistance coefficient (see Ref. [26]) given by

$$R_{ph} = 4/C_{ph,m}v_{ph,m} + 4/C_{ph}v_{ph}, \tag{41}$$

Note that the result (41) was established in the case of diffusive surfaces [31]. The subscript "ph,m" stands for the phonon contribution in the bulk matrix, while the subscript "ph" denotes the phonon contribution in the nanoparticle (also equal to the one in the nanofilm in the previous section). It is important to note that equation (39) stands for the effective thermal conductivity that would be measured in a nanocomposite composed out of a bulk matrix and a volume fraction of nanoparticles; it is thus a combination of macroscopic and microscopic heat transfer phenomena. In thermoelectric devices, the combination of macroscopic and microscopic phenomena can lead to different results as the nanoparticle volume fraction changes. For low volume fractions, the macroscopic heat transfer will be more important, while for higher volume fractions, the microscopic one will take the lead. The electron contribution follows the same path, defining the electron thermal conductivity, electric conductivity and the electron contribution of the effective thermal conductivity

$$k_{e,m} = \frac{1}{3}\left(C_{e,m}v_{e,m}\Lambda_{e,m}\right)|_{T_{ref}}, \tag{42}$$

$$\sigma_m = \frac{k_{e,m}}{LT}, \tag{43}$$

$$k_e^{eff} = k_{e,m}\frac{2k_{e,m}+(1+2\alpha_e)k_{e,\mathcal{N}}+2\varphi\left[(1-\alpha_e)k_{e,\mathcal{N}}-k_{e,m}\right]}{2k_{e,m}+(1+2\alpha_e)k_{e,\mathcal{N}}-\varphi\left[(1-\alpha_e)k_{e,\mathcal{N}}-k_{e,m}\right]}, \tag{44}$$

respectively. In Eq. (44), $k_{e,\mathcal{N}}$ is given by Eq. (24) and α_e is obtained from α_{ph} from Eq. (40), by replacing $k_{ph,m}$ by $k_{e,m}$ (42) and R_{ph} by $R_e = 4/C_{e,m}v_{e,m} + 4/C_e v_e$. The total effective thermal conductivity is given by

$$k_{tot}^{eff} = k_{ph}^{eff} + k_e^{eff}, \tag{45}$$

while the effective electric conductivity is expressed as

$$\sigma^{eff} = \frac{k_e^{eff}}{LT}. \tag{46}$$

As for the Seebeck coefficient, we cannot take a volumetric average since this means neglecting the effect of size. Also, we need to redefine the Seebeck coefficient for the nanocomposite:

$$S_m = \frac{n_{n,m}\mu_n S_{n,m}^* + n_{p,m}\mu_p S_{p,m}^*}{n_{n,m}\mu_n + n_{p,m}\mu_p}, \tag{47a}$$

$$S_{\mathcal{N}} = \frac{n_{n,\mathcal{N}}\mu_n S_{n,\mathcal{N}}^* + n_{p,\mathcal{N}}\mu_p S_{p,\mathcal{N}}^*}{n_{n,\mathcal{N}}\mu_n + n_{p,\mathcal{N}}\mu_p}, \tag{47b}$$

with S_m the Seebeck coefficient of the matrix (the bulk material) and $S_{\mathcal{N}}$ the Seebeck coefficient of the nanoparticle. Furthermore,

$$S_{x,y}^* = (-1)^z \frac{8\pi^2 {k_B}^2}{3e_c h^2} m_x^* T \left(\frac{\pi}{3n_{x,y}}\right)^{2/3}, \tag{48}$$

where the subscript x denotes whether it concerns the Seebeck coefficient of electrons ($x = n$ and $z = 1$) or that of holes ($x = p$ and $z = 2$) and the subscript y denotes whether it concerns the bulk material ($y = m$) or the nanoparticle ($y = \mathcal{N}$). If the material is only of the n-type then

$S_{\mathcal{N}} = S^*_{n,\mathcal{N}}$ (for the nanoparticle) and $S_m = S^*_{n,m}$ (for the bulk matrix), while a p-type material would have $S_{\mathcal{N}} = S^*_{p,\mathcal{N}}$ (for the nanoparticle) and $S_m = S^*_{p,m}$ (for the bulk matrix). In this definition of the Seebeck coefficient, we need again to pay attention to the carrier concentration of the holes and electrons, but this time because of two reasons: the nanoparticle size is at nanoscale and they are embedded in another material. This causes not only the scattering [23] of the carriers within the nanoparticles but also at the nanoparticle-matrix boundary, which influences the carrier concentration within the matrix as well. We assume again, as in the previous subsection, that the variation of the carrier concentrations (and its scattering behavior) also follows that of the electric conductivity (which follows that of the thermal conductivity, described by EIT) for both the nanoparticles (see Eq. (26)) and the bulk matrix. From Eqs. (26), (28), (42) and (43), we have

$$n_{x,\mathcal{N}}\mu_x \sim \sigma_{\mathcal{N}} = \frac{3\sigma^0}{4\pi^2 K n_e{}^2}\left[\frac{2\pi K_{\ e}}{arctan(2\pi K_{\ e})} - 1\right], \tag{49}$$

$$n_{x,m}\mu_x \sim \sigma_m = \frac{1}{3LT}\left(C_{e,m} v_{e,m} \Lambda_{e,m}\right)|_{T_{ref}}. \tag{50}$$

As noticed earlier, we take the mobility to be dependent on the carrier concentration as $\mu_x \sim n_x^{-1/3}$, which leads to:

$$n_{x,\mathcal{N}}^{2/3} \sim \sigma_{\mathcal{N}}, \tag{51a}$$

$$n_{x,m}^{2/3} \sim \sigma_m. \tag{51b}$$

This leads finally to

$$n_{x,\mathcal{N}} = n_{x,0}\left(\frac{\sigma_{\mathcal{N}}}{\sigma^0}\right)^{3/2} = n_{x,0}\left(\frac{k_{e,\mathcal{N}}}{k_e^0}\right)^{3/2}, \tag{52a}$$

$$n_{x,m} = n_{x,0}\left(\frac{\sigma_m}{\sigma_m^0}\right)^{3/2} = n_{x,0}\left(\frac{k_{e,m}}{k_{e,m}^0}\right)^{3/2} = n_{x,0}\left(\frac{\Lambda_{e,m}}{\Lambda_{e,b,m}}\right)^{3/2}, \tag{52b}$$

with σ_m^0 and $k_{e,m}^0$ the electric conductivity and the electron thermal conductivity, respectively, of the matrix bulk material (without taking into account the effect of electron scattering due to the nanoparticles, i.e. $\Lambda_{e,m} \equiv \Lambda_{e,b,m}$ and $\varphi = 0$).

The size dependency of the Seebeck coefficient for nanofilms has been taken into account via the carrier concentration. For nanocomposites, however, it is quite different, since the two materials are present, one of which is at nanoscales. This will lead to an effective Seebeck coefficient. However, the Seebeck coefficient is not to be taken size-dependent in the same way as the thermal conductivity, since Eqs. (6c) and (7c) suggests that S and σ are to be evaluated together when it comes to the extended thermodynamic approach of nanocomposite thermoelectric devices in this work (assuming $\Lambda_I \equiv \Lambda_e$). Therefore, with Eq. (25) (keeping in mind Eq. (26)), we have

$$(S\sigma)_{\mathcal{N}} = \frac{S_{\mathcal{N}}}{LT} k_{e,\mathcal{N}}. \tag{53}$$

For the matrix, an analogous expression can be obtained:

$$(S\sigma)_m = \frac{S_m}{LT} k_{e,m}, \tag{54}$$

Then we have in analogy with Eq. (44)

$$(S\sigma)^{eff} = (S\sigma)_m \frac{2(S\sigma)_m + (1+2\alpha_e)(S\sigma)_{\mathcal{N}} + 2\varphi[(1-\alpha_e)(S\sigma)_{\mathcal{N}} - (S\sigma)_m]}{2(S\sigma)_m + (1+2\alpha_e)(S\sigma)_{\mathcal{N}} - \varphi[(1-\alpha_e)(S\sigma)_{\mathcal{N}} - (S\sigma)_m]}. \quad (55)$$

The effective Seebeck coefficient S^{eff} and the effective power factor PF^{eff} can then be easily obtained a posteriori, by defining

$$S^{eff} = (S\sigma)^{eff}/\sigma^{eff}, \quad (56)$$
$$PF^{eff} = S^{eff\,2}\sigma^{eff} = (S\sigma)^{eff\,2}/\sigma^{eff}. \quad (57)$$

Finally, with the preceding equations, we can obtain the effective non-dimensional figure of merit for nanocomposites:

$$ZT^{eff} = T\frac{(S^{eff})^2\sigma^{eff}}{k_{ph}^{eff}+k_e^{eff}} = T\frac{(S\sigma)^{eff\,2}/\sigma^{eff}}{k_{ph}^{eff}+k_e^{eff}} = LT^2\frac{(S\sigma)^{eff\,2}}{k_e^{eff}\left(k_{ph}^{eff}+k_e^{eff}\right)}. \quad (58)$$

The model presented in section 2.3 will be applied for nanofilms of Bismuth (Bi) and p-type BismuthTelluride (Bi_2Te_3). This model is again extended in section 2.4 describing the thermoelectric properties of nanocomposites that have one dimension at nanoscale.

4. Mathematical model for the extension to thin film nanocomposites

In this section we extend the model from the previous subsection to thermoelectric systems in the form of nanofilms composed out of nanocomposites (of course, the film thickness should be larger than the particle diameters). The description of the conductivities and the components of the figure of merit for the nanoparticles will remain the same as the previous. The differences are the parts that describe the matrix which is now also at nanoscale in contrast to the previous subsection. The new nanoscale matrix phonon thermal conductivity, $k_{ph,m}^{\mathcal{N}}$, will be given by Eq. (23), where k_{ph}^0 should now be given by Eq. (36):

$$k_{ph,m}^{\mathcal{N}} = \frac{3k_{ph,m}}{4\pi^2 Kn_{ph}^{\mathcal{N}\,2}}\left[\frac{2\pi Kn_{ph}^{\mathcal{N}}}{arctan(2\pi Kn_{ph}^{\mathcal{N}})} - 1\right] = \frac{C_{ph,m}v_{ph,m}\Lambda_{ph,m}}{4\pi^2 Kn_{ph}^{\mathcal{N}\,2}}\left[\frac{2\pi Kn_{ph}^{\mathcal{N}}}{arctan(2\pi Kn_{ph}^{\mathcal{N}})} - 1\right], \quad (59)$$

with $Kn_{ph}^{\mathcal{N}} = \Lambda_{ph,b,m}/\delta_{m,s}^{\mathcal{N}}$ the phonon Knudsen number of the nanoscale matrix, where $\delta_{m,s}^{\mathcal{N}} = \delta_m^{\mathcal{N}}(1+s)/(1-s)$, with $\delta_m^{\mathcal{N}}$ the film thickness of the nanocomposite. The nanoscale effective phonon thermal conductivity, $k_{ph}^{\mathcal{N},eff}$, is then, in analogy with Eq. (39), given by

$$k_{ph}^{\mathcal{N},eff} = k_{ph,m}^{\mathcal{N}}\frac{2k_{ph,m}^{\mathcal{N}} + \left(1+2\alpha_{ph}^{\mathcal{N}}\right)k_{ph,\mathcal{N}} + 2\varphi\left[\left(1-\alpha_{ph}^{\mathcal{N}}\right)k_{ph,\mathcal{N}} - k_{ph,m}^{\mathcal{N}}\right]}{2k_{ph,m}^{\mathcal{N}} + \left(1+2\alpha_{ph}^{\mathcal{N}}\right)k_{ph,\mathcal{N}} - \varphi\left[\left(1-\alpha_{ph}^{\mathcal{N}}\right)k_{ph,\mathcal{N}} - k_{ph,m}^{\mathcal{N}}\right]}, \quad (60)$$

with $k_{ph,\mathcal{N}}$ given by Eq. (23). In expression (60), $\alpha_{ph}^{\mathcal{N}}$ is given by Eq. (40), but replacing $k_{ph,m}$by $k_{ph,m}^{\mathcal{N}}$. In analogy with Eq. (60), the electron contribution of the thermal conductivity is given by

$$k_e^{\mathcal{N},eff} = k_{e,m}^{\mathcal{N}}\frac{2k_{e,m}^{\mathcal{N}} + \left(1+2\alpha_e^{\mathcal{N}}\right)k_{e,\mathcal{N}} + 2\varphi\left[\left(1-\alpha_e^{\mathcal{N}}\right)k_{e,\mathcal{N}} - k_{e,m}^{\mathcal{N}}\right]}{2k_{e,m}^{\mathcal{N}} + \left(1+2\alpha_e^{\mathcal{N}}\right)k_{e,\mathcal{N}} - \varphi\left[\left(1-\alpha_e^{\mathcal{N}}\right)k_{e,\mathcal{N}} - k_{e,m}^{\mathcal{N}}\right]}, \quad (61)$$

with $k_{e,\mathcal{N}}$ given by Eq. (24). In expression (61), $\alpha_e^{\mathcal{N}}$ is obtained from Eq. (40), by replacing R_{ph} by $R_e = 4/C_{e,m}v_{e,m} + 4/C_e v_e$ and $k_{e,m}$ by $k_{e,m}^{\mathcal{N}}$, the latter being given, in analogy with Eq. (59) by

$$k_{e,m}^{\mathcal{N}} = \frac{C_{e,m}v_{e,m}\Lambda_{e,m}}{4\pi^2 {Kn_e^{\mathcal{N}}}^2}\left[\frac{2\pi Kn_e^{\mathcal{N}}}{arctan(2\pi Kn_e^{\mathcal{N}})} - 1\right], \tag{62}$$

with $Kn_e^{\mathcal{N}} = \Lambda_{e,b,m}/\delta_{m,s}^{\mathcal{N}}$ the electron Knudsen number of the nanoscale matrix, where $\delta_{m,s}^{\mathcal{N}}$ is here again the speculate film thickness. The total nanoscale effective thermal conductivity is given by

$$k_{tot}^{\mathcal{N},eff} = k_{ph}^{\mathcal{N},eff} + k_e^{\mathcal{N},eff}, \tag{63}$$

while the nanoscale effective electric conductivity is expressed as (in analogy with Eq. (46))

$$\sigma^{\mathcal{N},eff} = \frac{k_e^{\mathcal{N},eff}}{LT}. \tag{64}$$

As for the Seebeck coefficient, we have in analogy with Eq. (55)

$$(S\sigma)^{\mathcal{N},eff} = (S\sigma)_m^{\mathcal{N}} \frac{2(S\sigma)_m^{\mathcal{N}} + \left(1+2\alpha_e^{\mathcal{N}}\right)(S\sigma)_{\mathcal{N}} + 2\varphi\left[\left(1-\alpha_e^{\mathcal{N}}\right)(S\sigma)_{\mathcal{N}} - (S\sigma)_m^{\mathcal{N}}\right]}{2(S\sigma)_m^{\mathcal{N}} + \left(1+2\alpha_e^{\mathcal{N}}\right)(S\sigma)_{\mathcal{N}} - \varphi\left[\left(1-\alpha_e^{\mathcal{N}}\right)(S\sigma)_{\mathcal{N}} - (S\sigma)_m^{\mathcal{N}}\right]}, \tag{65}$$

with $(S\sigma)_{\mathcal{N}}$ given by Eq. (53), $\alpha_e^{\mathcal{N}}$ defined under Eq. (61) and $(S\sigma)_m^{\mathcal{N}}$ derived from $(S\sigma)_m$ (see Eq. (54)) by replacing $k_{e,m}$ by $k_{e,m}^{\mathcal{N}}$ (see Eq. (62)) and $S_m$by $S_m^{\mathcal{N}}$. Note that $(S\sigma)_m^{\mathcal{N}} \equiv S_m^{\mathcal{N}}\sigma_m^{\mathcal{N}}$, with $\sigma_m^{\mathcal{N}}$ and $S_m^{\mathcal{N}}$ the nanoscale electric conductivity and Seebeck coefficient of the matrix, given by, respectively,

$$\sigma_m^{\mathcal{N}} = \frac{k_{e,m}^{\mathcal{N}}}{LT}. \tag{66}$$

$$S_m^{\mathcal{N}} = \frac{n_{n,m}\mu_n S_{n,m}^{*,\mathcal{N}} + n_{p,m}\mu_p S_{p,m}^{*,\mathcal{N}}}{n_{n,m}\mu_n + n_{p,m}\mu_p}, \tag{67}$$

where

$$S_{x,y}^{*,\mathcal{N}} = (-1)^z \frac{8\pi^2 {k_B}^2}{3e_c h^2} m_x^* T \left(\frac{\pi}{3n_{x,y}^{\mathcal{N}}}\right)^{2/3}, \tag{68}$$

with $n_{x,y}^{\mathcal{N}}$ defined (in analogy with Eqs. (52)). In the case of the nanoparticles $n_{x,y}^{\mathcal{N}} = n_{x,\mathcal{N}}$ (Eq. (52a)). In the case of the nanoscale matrix $n_{x,y}^{\mathcal{N}} = n_{x,m}^{\mathcal{N}}$ (keeping in mind the definitions of x, y and z and the explanation of using Eq. (67), all to be consulted in the text under Eq. (48)) given by

$$n_{x,m}^{\mathcal{N}} = n_{x,0}\left(\frac{\sigma_m^{\mathcal{N}}}{\sigma_m^0}\right)^{3/2} = n_{x,0}\left(\frac{k_{e,m}^{\mathcal{N}}}{k_{e,m}^0}\right)^{3/2}. \tag{69}$$

The effective nanoscale Seebeck coefficient $S^{\mathcal{N},eff}$ and the effective nanoscale power factor $PF^{\mathcal{N},eff}$ can then be easily obtained a posteriori, by defining

$$S^{\mathcal{N},ef} = (S\sigma)^{\mathcal{N},eff}/\sigma^{\mathcal{N},eff}, \quad (70)$$

$$PF^{\mathcal{N},eff} = S^{\mathcal{N},eff^2}\sigma^{\mathcal{N},eff} = (S\sigma)^{\mathcal{N},eff^2}/\sigma^{\mathcal{N},eff}. \quad (71)$$

Finally the nanoscale effective non-dimensional figure of merit for nanofilms composed out of nanocomposites is given by

$$ZT^{\mathcal{N},ef} = T\frac{\left(S^{\mathcal{N},eff}\right)^2\sigma^{\mathcal{N},eff}}{k_{ph}^{\mathcal{N},eff}+k_e^{\mathcal{N},eff}} = T\frac{(S\sigma)^{\mathcal{N},eff^2}/\sigma^{\mathcal{N},eff}}{k_{ph}^{\mathcal{N},eff}+k_e^{\mathcal{N},eff}} = LT^2\frac{(S\sigma)^{\mathcal{N},eff^2}}{k_e^{\mathcal{N},eff}\left(k_{ph}^{\mathcal{N},eff}+k_e^{\mathcal{N},eff}\right)}. \quad (72)$$

5. Material properties for Bi and Bi_2Te_3

Historically, Bismuth was the first material showing substantial thermoelectric coefficients [32] and BismuthTelluride is one of the best performing thermoelectric materials at room temperature [33]. As such, the choice of these materials is actually well justified. Bismuth is a semi-metal where the electric conductivity passes via both hole and electron mobility. We can obtain the electric conductivity via Eq. (22). The hole (μ_p) and electron (μ_n) mobilities are 1 and 0.4 m^2/Vs, respectively [34]. The carrier concentrations of the holes and electrons are each $3.5*10^{24}$ m^{-3} [34]. This gives an electric conductivity σ^0 of $7.85*10^5$ $\Omega^{-1}m^{-1}$. The Lorentz number can be obtained by Eq. (21) to be $2.44*10^{-8}$ W Ω/K^2. The electron thermal conductivity is then given by $k_e^0 \equiv \sigma^0 LT$, obtaining 5.75 W/Km. The electron thermal velocity is given by $\sqrt{3k_BT/m^*}$ [35]. With $m^* = 0.16m^0$ [36] for the electrons (the same holds for the holes), we find an electron thermal velocity of $2.92*10^5$ m/s. The electron mean free path is 0.67 nm [37,38]. This gives with the electron version of Eq. (2) an electron specific heat capacity of 0.088 MJ/m^3K. Assuming that the total specific heat capacity (1.21 MJ/m^3K [39]) is the sum of the electron and phonon ones, we can find the phonon specific heat capacity of 1.12 MJ/m^3K. The phonon mean free path is 3.0 nm [40]. Via Eq. (2), we can find a phonon group velocity of 1980 m/s. This value corresponds nicely with the value of 1790 m/s, proposed by [37]. This gives finally all the electron and phonon material properties needed for the calculation of the effective thermal conductivities for Bismuth. In order to calculate the figure of merit, we still need to calculate the Seebeck coefficient. Using Eqs. (25) and (26), we can find a bulk Seebeck coefficient of 139 µV/K for Bismuth. A resume of these properties are given in Table 1.

As for p-type (the electric conductivity passes only via the mobility of holes) BismuthTelluride the electron (C_e, v_e and $\Lambda_{e,b}$) and phonon (C_{ph}, v_{ph} and $\Lambda_{ph,b}$) material properties are given by [41]. As for the Seebeck coefficient we use Eq. (25) with $x = p$ and $m^* = 1.25m^0$ (using the six-valley model) [42] for the holes (p-type) and obtain finally a bulk value of 188 µV/K for Bi_2Te_3. The mobility is $420*10^{-4}$ m^2/Vs [43] and the electric conductivity can be found by $\sigma^0 = k_e^0/LT$, with $k_e^0 = \frac{1}{3}C_e v_e \Lambda_{e,b}$, so that the electric conductivity is found to be $3.28*10^5$ $\Omega^{-1}m^{-1}$. With this we can find the hole carrier concentration from Eq. (22) to be $4.87*10^{25}$ m^{-3}. A resume of these properties are given in Table 1. Table 2 shows the values of the used physical constants.

Table 1: Electron and phonon material properties of Bi and Bi_2Te_3 at T = 300K.

Material	Electron			Phonon			Carrier		
	C_e [MJ/ m^3K]	v_e [km/s]	$\Lambda_{e,b}$ [nm]	C_{ph} [MJ/ m^3K]	v_{ph} [km/s]	$\Lambda_{ph,b}$ [nm]	$n_{p,m}$ [10^{24} m^{-3}]	$n_{n,m}$	S_m [µV/K]
Bi	0.088	292	0.67	1.12	1.98	3.0	3.5	3.5	59
Bi_2Te_3	1.01	7.83	0.91	0.19	8.43	3.0	48.7	–	188

Table 2: Physical constants at T = 300K.

Physical constant	k_B [J/K]	h [Js]	e_c [C]	L [W Ω/K^2]	m^0 [kg]
Value	$1.38*10^{-23}$	$6.626*10^{-34}$	$1.602*10^{-19}$	$2.44*10^{-8}$	$9.11*10^{-31}$

6. Results and discussion

6.1 Thermoelectric properties of nanofilms of Bi and Bi_2Te_3

Fig. 1 presents the phonon, electron and total thermal conductivities (also for several specularities), electric conductivity and the dimensionless figure of merit for Bi and Bi_2Te_3.

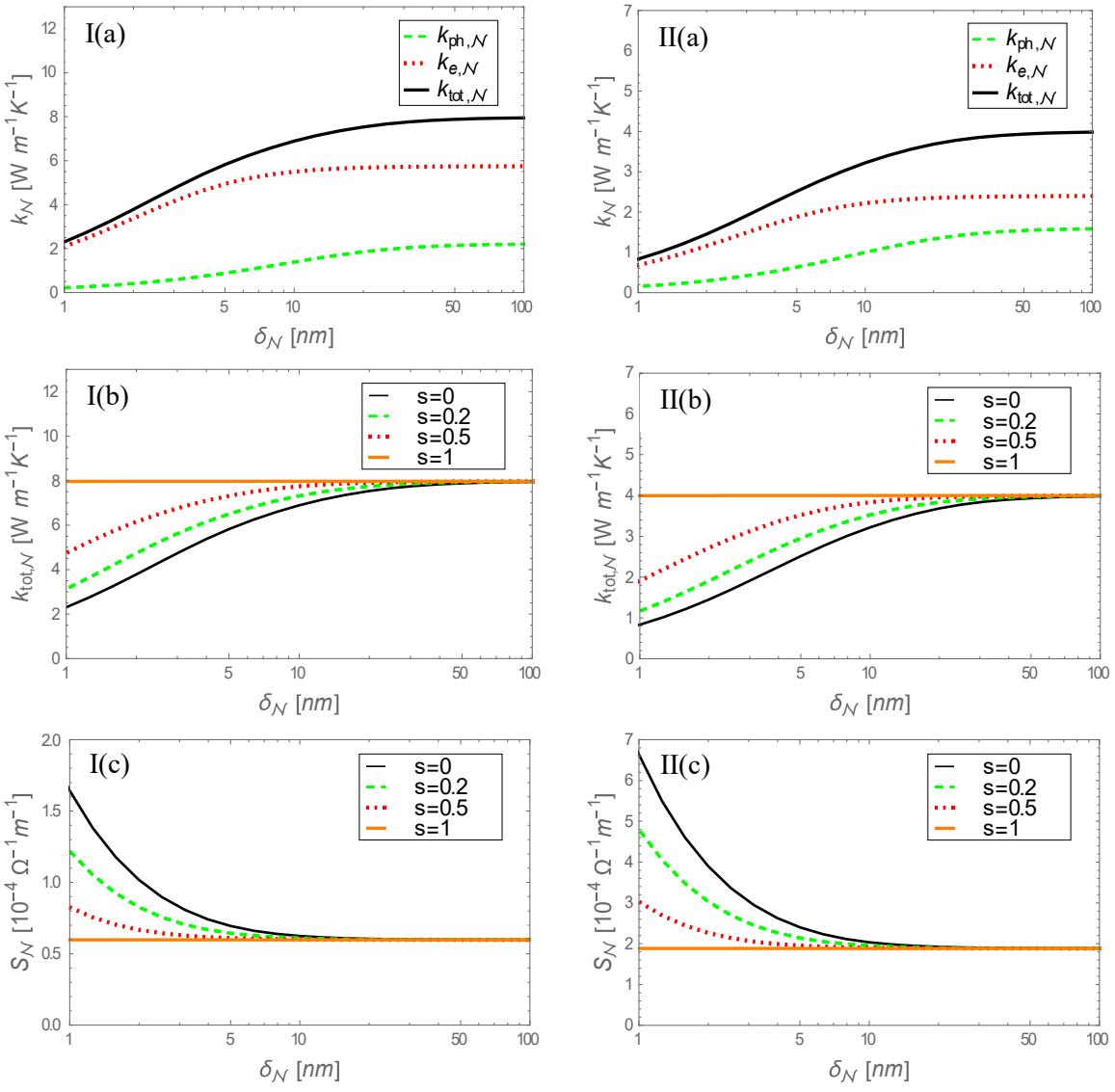

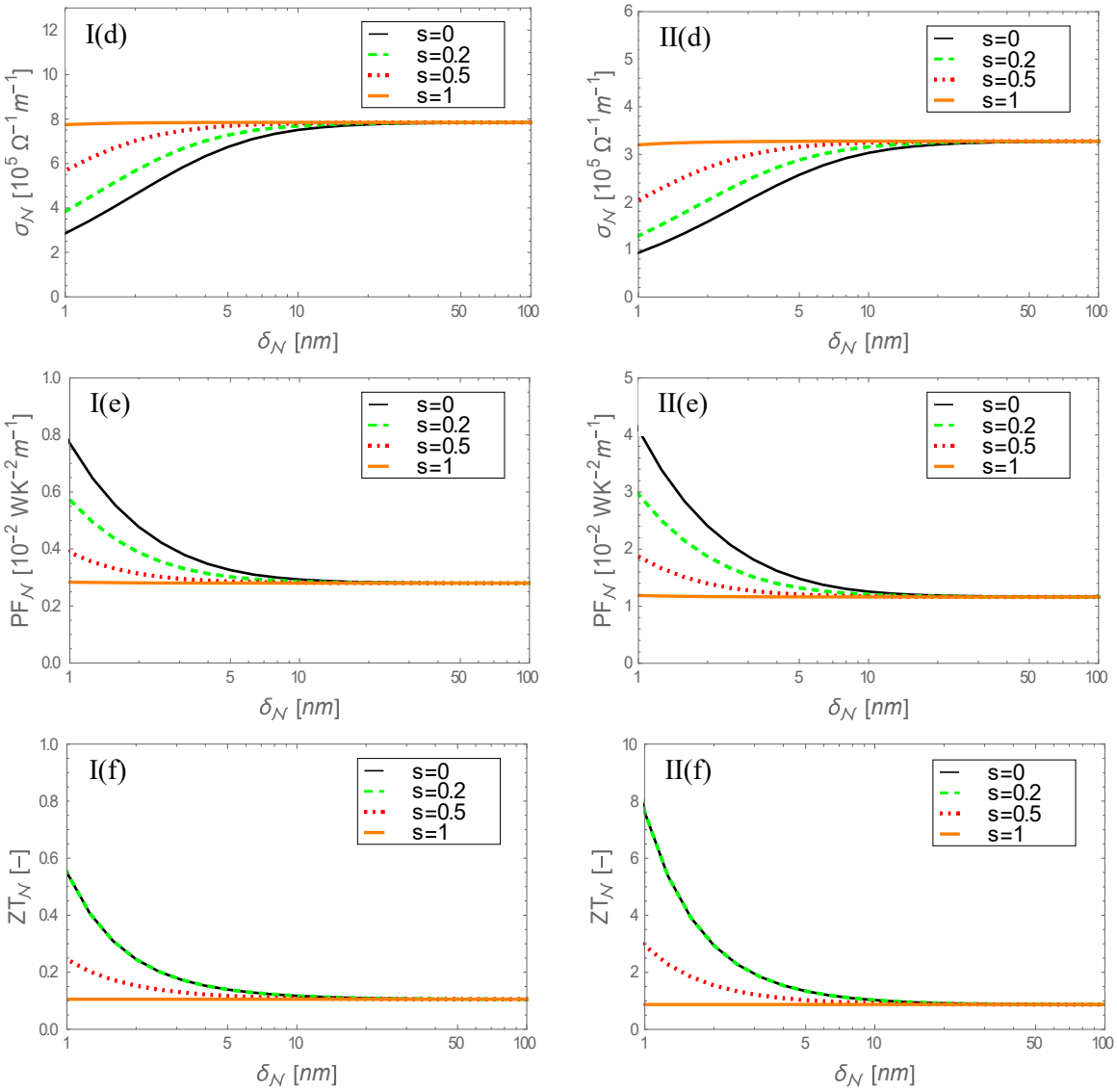

Fig. 1: Dependence on the film thickness $\delta_{\mathcal{N}}$ of Bi (left, indicated by I) and Bi_2Te_3 (right, indicated by II) of (a) the phonon, electric and total thermal conductivity ($k_{ph,\mathcal{N}}$, $k_{e,\mathcal{N}}$ and $k_{tot,\mathcal{N}}$) for $s = 0$ and, (b) the total thermal conductivity $k_{tot,\mathcal{N}}$, (c) the Seebeck coefficient $S_{\mathcal{N}}$, (d) the electric conductivity $\sigma_{\mathcal{N}}$, (e) the power factor $PF_{\mathcal{N}}$ and (f) the dimensionless figure of merit $ZT_{\mathcal{N}}$, for $s = 0, 0.2, 0.5$ and 1.

We start the discussion first for $s = 0$. From Fig. 1(Ia,Ib,IIa,IIb), we can see clearly that the thermal conductivities for both considered nanofilms (Bi and Bi_2Te_3) decrease considerably for thicknesses below 50 nm. This is due to the scattering effect of the phonons and electrons. As the film thickness decreases, the ballistic effects (phonons colliding with boundaries of which the dimensions approach that of the mean free paths). The scattering effect has clear influences on the scattering of the carriers translated into a sharp increase of the Seebeck coefficient (see Eq. (24)) in Fig. 1(Ic,IIc). The electric conductivity follows the behavior of the electron thermal conductivity (see Fig. Id,IId) for the same reasons, i.e. the scattering of the electrons. Fig. 1(Ie,IIe) shows the power factor, which increases as the nanofilm thickness decreases. Finally Fig. 1(If,IIf) shows the figure of merit, which shows us that the decreasing thermal conductivity and the increasing Seebeck coefficient result into an increased figure of merit. Note the relatively high value for the figure of merit in Fig. 1(IIf). It should be mentioned that a value of $ZT_{\mathcal{N}} = 8$ (for $s = 0$ and 0.2) is quite on the high side. It is still shown here as an extrapolation

for purposes of mathematical interest, showing to what extent nanofilms can increase the figure of merit. We can also see that the electron thermal conductivity decreases less than the phonon one, which also contributes to increased figure of merit. As far as concerns the difference between Bi and Bi_2Te_3, it can be said that they show the same behaviour. The results only differ quantitatively. Bi_2Te_3 presents a higher Seebeck coefficient and power factor than Bi, resulting into higher figure of merits. It is interesting to note that the values at $s \to 1$ are constant. This can be interpreted in two ways. Firstly, for $s \to 1$, the electron and phonon scattering occurs on a so-called smooth surface so that the incoming phonons and electrons leave the boundary of the nanofilm at the same angle. In other words, the boundaries are specular. This results into zero scattering and the heat transfer occurs fully, so that the thermal conductivities, electric conductivity and carriers do not undergo the effect of scattering and preserve their bulk values. As a consequence, also the Seebeck coefficient and power factor remain the same, resulting altogether in a constant figure of merit. Another interpretation is to say that for $s \to 1$, Eqs. (11a) and (11b) shows that $\ell_s \to \infty$. This means that the nanofilm behaves as if it were a macrofilm with bulk properties. As far as goes the results for $0 < s < 1$, they show intermediate tendencies between those of $s = 0$ and $s \to 1$, as expected. Now we have seen the influence of the film dimension on the thermoelectric properties, we assess the influence of adding nanoparticles in the next subsection.

6.2 Thermoelectric properties of nanocomposites of Bi nanoparticles in Bi_2Te_3 and of Bi_2Te_3 nanoparticles in Bi

Fig. 2 presents the phonon, electron and total thermal conductivities (also for several specularities), electric conductivity and the dimensionless figure of merit as a function of the volume fraction of nanoparticles for two systems: left, Bi nanoparticles embedded in Bi_2Te_3, and, right, Bi_2Te_3 nanoparticles embedded in Bi. The size of the nanoparticles is 1 nm.

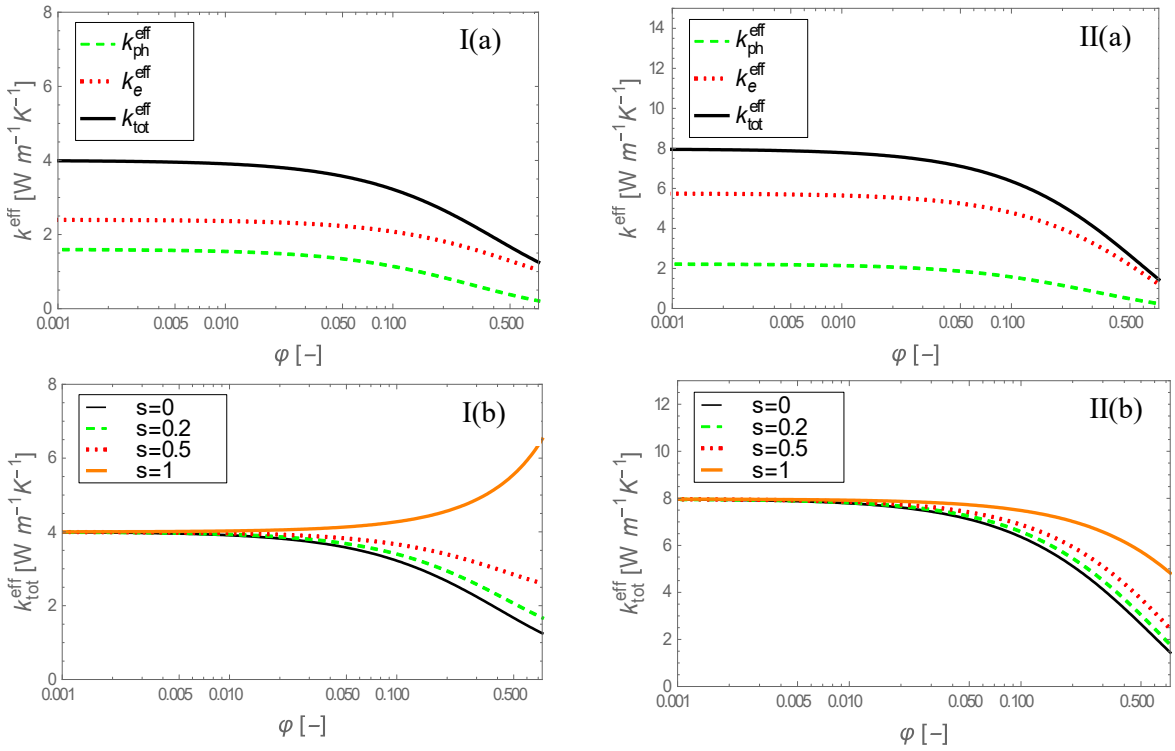

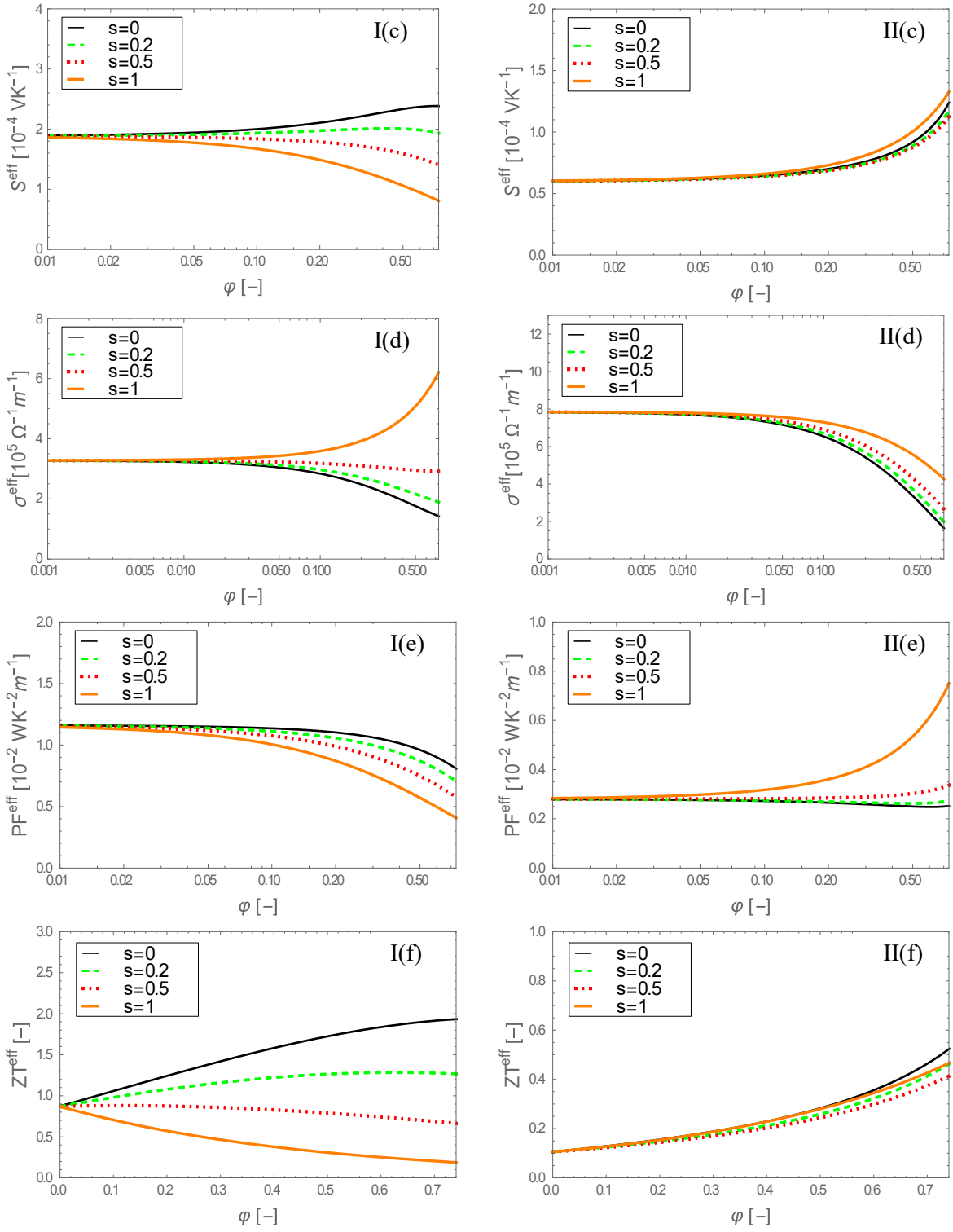

Fig. 2: Dependence on the volume fraction φ of, respectively, 1 nm Bi nanoparticles in a matrix of Bi_2Te_3 (left, indicated by I) and 1 nm Bi_2Te_3 nanoparticles in a matrix of Bi (right, indicated by II) of: (a) the phonon, electric and total effective thermal conductivity (k_{ph}^{eff}, k_e^{eff} and k_{tot}^{eff}, respectively) for $s = 0$, and (b) the total effective thermal conductivity k_{tot}^{eff}, (c) the effective Seebeck coefficient S^{eff}, (d) the effective electric conductivity σ^{eff}, (e) the effective power factor PF^{eff} and (f) the dimensionless effective figure of merit ZT^{eff}, for $s = 0, 0.2, 0.5$ and 1.

Again, we start with discussing the results for $s = 0$. From Fig. 2(Ia,Ib,IIa,IIb), we can see that the effective thermal conductivities decrease as the volume fraction of the nanoparticles increase. The reason of this decrease is twofold. Firstly, due to an increase of the nanoparticles, the mean free path of phonons and electrons in the host matrix decreases (see Eqs. (38) and (42)) and so does the overall mean free path of phonons and electrons (Eq. (37)). This causes the effective thermal conductivity of the matrix to decrease (Eq. (36) for the phonon contribution and Eq. (42) for the electron one). Secondly, due to the small size (1 nm) of the nanoparticles, the phonon and electron scattering cause a considerable decrease of the nanoparticle effective phonon thermal conductivity (Eq. (23) and for the electron contribution, see Eq. (24)). The effective electric conductivity follows, for the same reasons, the behavior of the thermal one (see Fig. 2(Id,IId)). As for the effective Seebeck coefficient in Fig. 2(Ic,IIc), it increases as the volume fraction increases. However, this increase is not as strong as the decrease of the thermal and electric conductivities. This can be explained by considering that the scattering effect on the effective Seebeck coefficient has two sources. The first can be understood via the principles of EIT (see Eq. (7c)), which is explicitly expressed in Eq. (55) for the effective Seebeck coefficient. Following Eq. (55), the effective Seebeck coefficient should decrease due to the scattering effect, in analogy with the effective thermal conductivity (Eqs. (39) and (44)). The second, however, shows via Eq. (48) that the effective Seebeck coefficient is inversely proportional to the carrier concentration by a factor 2/3. The scattering behavior of the carriers is proportional to the decrease of the electric conductivity by a factor 3/2 (see Eqs. (51a) and (51b)). Therefore, the proportionality of the decreasing and increasing effects of the scattering process on the effective Seebeck coefficient compete with each other, so that the scattering effect is of more importance to the effective thermal conductivities. It appears, by the way, that the scattering process of the carriers is stronger than that expressed by Eq. (55), which explains the eventual increase of the effective Seebeck coefficient. Fig. 2(Ie,IIe) shows that the power factor decreases. This is due to the stronger decrease of the effective electric conductivity with respect to the increase of the effective Seebeck coefficient. This decreasing power factor results into a less strong increase of the figure of merit (see Fig. 2(If,IIf)) than was the case for the nanofilm in section 4.2, but increase nonetheless.

Now, comparing the two nanocomposites, we observe that the tendencies of all the parameters behave in the same way as a function of the volume fraction of nanoparticles. However, the dependency on the s parameter is not the same at all. As far as goes the Bi nanoparticles in Bi_2Te_3, we obtain expected results. A higher s-value results into a smoother surface, causing less scattering. It also can be interpreted by a higher particle radius (see Eqs. (11a) and (11c)), which at a given volume fraction decreases the particle-matrix interface, creating less obstacles for the phonons and electrons to transfer heat, increasing the thermal conductivity. However, in the case we have Bi_2Te_3 nanoparticles in a Bi matrix, we obtain surprising results. Of course, the lesser scattering effect of the nanoparticles and the particle-matrix interface play an important role, but there seems to be another effect that counteracts it. Fig. 2(IIb) shows that, even though for $s \to 1$ the effective thermal conductivity increases, this increase is less pronounced than in Fig. 2(Ib). The same goes for the effective thermal conductivity in Fig. 2(Id) and Fig. 2(IId), respectively. Moreover, being the most pronounced difference, the effective Seebeck coefficient at $s \to 1$ decreases in Fig. 2(Ic) and increases in Fig. 2 (IIc). Table 1 shows that bulk p-type Bi_2Te_3 has a much higher Seebeck coefficient than Bi. We have already said earlier that at $s \to 1$ bulk material values become important. Therefore, as the volume fraction increases at $s \to 1$, the effective Seebeck coefficient increases as well. In the fictive limit of $\varphi \to 1$, which is not possible here, since we assume that the nanoparticles are undeformable spheres that do not merge with other ones (at maximum packing $\varphi_{max} = \pi/\sqrt{18}$), we obtain the bulk value for Bi_2Te_3, while at $\varphi = 0$, we obtain that of Bi. The sum of all these effects

gives eventually the result that the figure of merit in Fig. 2(IIf) is hardly influence by the s-value.

We have seen that the s-parameter influences greatly the thermoelectric properties and we said that one of the interpretations is higher nanoparticle radii for higher s-values. The nanoparticle radius used for the results in Fig. 2 is 1 nm. We are therefore interested to assess the influence of the nanoparticle radius on the figure of merit. For this purpose, Fig. 3 presents the dimensionless effective figure of merit as a function of the inverse phonon Knudsen number $Kn_{ph}^{-1}{\sim}r_p$ at $s = 0$ and for volume fractions $\varphi = 0, 0.2, 0.4$ and 0.7. Note that doing the same as a function of the inverse electron Knudsen number mounts to the same tendency since $Kn_e = Kn_{ph}\Lambda_e/\Lambda_{ph}$. It should be mentioned that, regarding the values of the mean free paths in Table 2, the phonon Knudsen number cannot realistically be of order 10 or larger (the nanoparticle radii should be significantly larger than the atom sizes). So, in real-life situations, for the materials in this work, $Kn_{ph} \ll 10$, or $Kn_{ph}^{-1} \gg 0.1$. Nonetheless, we would like to perform a dimensionless analysis and investigate the behavior of the figure of merit with respect to nanoparticle size. Therefore, we used a much larger range of Kn_{ph}^{-1}, so that we capture all the phenomena for mathematical interest. This point is related to the results of both Fig. 1(IIf) ($ZT_{\mathcal{N}} = 8$) and Fig. 3(a) ($ZT^{eff} = 15$ for $\varphi = 0.7$). As such, the results will indeed be qualitatively valid for other materials which have much higher mean free paths.

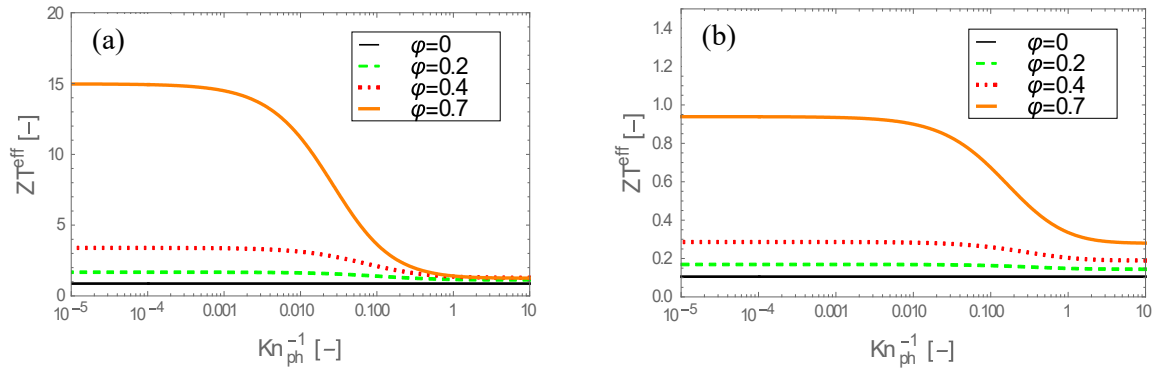

Fig. 3: Dependence on the inverse phonon Knudsen number Kn_{ph}^{-1}, for several volume fractions, of the effective dimensionless figure of merit ZT^{eff}, for (a) Bi nanoparticles in a matrix of Bi_2Te_3 and (b) Bi_2Te_3 nanoparticles in a matrix of Bi.

Fig. 3 shows that the nanoparticle size influences greatly the figure of merit (and thus the thermoelectric properties). The value at $\varphi = 0$ is obviously the figure of merit value at $\delta_{\mathcal{N}} \to \infty$ or $s \to 1$ in Figs. 1(If) and 1(IIf). We can see that for increasing nanoparticle radius (decreasing Kn_{ph}), the figure of merit decreases and for decreasing nanoparticle radius (increasing Kn_{ph}), the figure of merit increases. This shows clearly the positive effect of nanocomposites on the figure of merit with respect to nanofilms for very large Knudsen numbers. It should be noted that the value of the figure of merit is higher in case of Fig. 3(a) than in case of Fig. 3(b). This is easily understood by noticing that Fig. 2(f) shows that Bi nanoparticles in a matrix of Bi_2Te_3 show already a higher figure of merit than Bi_2Te_3 nanoparticles in a matrix of Bi. For an even smaller nanoparticle (Kn_{ph}^{-1} decreases), this difference is more accentuated. Finally, it appears that with nanofilms, one may obtain even higher figure of merits as can be seen in the previous subsection. However, from a practical point of view, it can give problems in the robustness or production of the nanofilms if the thickness is too small. Therefore, we have extended our model in section 2.4 in order to investigate whether the combination of nanofilms and nanocomposites can increase the

thermoelectric performances of nanocomposites without decreasing too much the thickness of the nanocomposite material.

7. Discussion of extension towards thin films of Bi-Bi_2Te_3 nanocomposites: a Gedankenexperiment

Fig. 4 shows the effect of the film thickness of the nanocomposites considered in the previous section. Here the nanoparticles have a radius of 1 nm, $s = 0$ and the results are presented for volume fractions $\varphi = 0, 0.2, 0.4$ and 0.7.

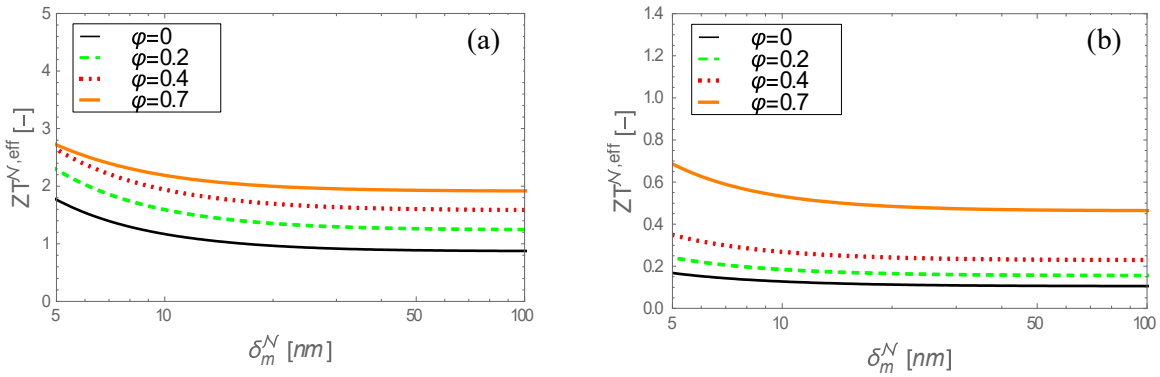

Fig. 4: Dependence on the nanocomposite film thickness $\delta_m^{\mathcal{N}}$ of, respectively, (a) 1 nm Bi nanoparticles in a matrix of Bi_2Te_3 and (b) 1 nm Bi_2Te_3 nanoparticles in a matrix of Bi (b) the dimensionless effective figure of merit $ZT^{\mathcal{N},eff}$, for volume fractions $\varphi = 0, 0.2, 0.4$ and 0.7.

From the results of Fig. 4, we can see indeed that decreasing the film thickness of the nanocomposites, we can improve further more the figure of merit. The improvement is not large but still significant. This weak improvement can be understood due to the minimum film thickness considered, i.e. $\delta_{m,min}^{\mathcal{N}} = 5$ nm, which is larger than both the phonon and electron mean free paths (though still in the same order of magnitude). Therefore the Knudsen number is smaller than one. As shown in Fig. 3, this leads to poorer thermoelectric properties. We did not consider smaller thicknesses, since the nanoparticle size is 2 nm (radius of 1 nm). We consider that the thin film should be at least twice the particle size (four times the radius), so that the thin film is still considered as a composite. Let us imagine a smaller particle. We consider here only the case of a Bi nanoparticle embedded in a Bi_2Te_3 host matrix, as an example. A Bi atom has a van der Waals radius of approximately 0.2 nm. Let us consider, for the purposes of this Gedankenexperiment a Bi nanoparticle of radius 0.5 nm (smaller than both the phonon and electron mean free paths) within a host matrix Bi_2Te_3 of minimum thickness $\delta_{m,min}^{\mathcal{N}} = 2$ nm (smaller than the phonon mean free paths). We perform with these new settings the same calculations as in Fig. 4(a) and present the results in Fig. 5.

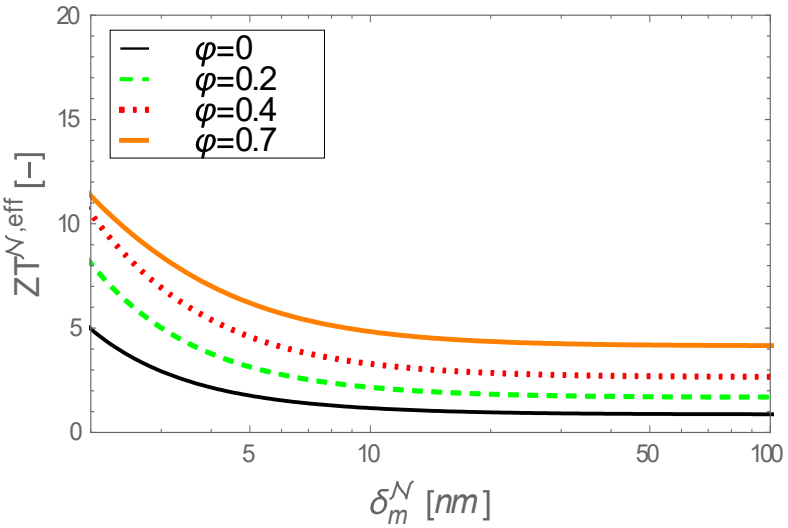

Fig. 5: The dimensionless figure of merit $ZT^{\mathcal{N},eff}$ of thin films of 0.5 nm Bi nanoparticles embedded in a Bi_2Te_3 host matrix as a function of the nanocomposite film thickness $\delta_m^{\mathcal{N}}$, for volume fractions $\varphi = 0, 0.2, 0.4$ and 0.7.

First of all, we can see high values of the figure of merit as high as $ZT^{\mathcal{N},eff} = 10$. As was mentioned in relation to Figs. 1(IIf) and 3(a), this value is rather high. However, for mathematical purposes it is interesting to make such an extrapolation, which allows appreciating the possibility of the configuration proposed in this section. Indeed, Fig. 5 shows that a much higher figure of merit can be obtained when combining the principle nanofilms and nanocomposites.

8. Conclusions

We present a mathematical model describing size-dependent subcontinuum thermoelectric properties based on extended irreversible thermodynamics, a new thermodynamic description suitable at nanoscale. It has been shown that a relatively simple closed-form formulation can capture complex size-dependent phenomena related to thermoelectric properties of nanofilms and nanocomposites. An extension has been presented towards nanofilms composed out of nanocomposites. The model includes size-dependent electron and phonon thermal conductivities, electric conductivity, Seebeck coefficient and carrier concentrations, all resulting into a size-dependent figure of merit. We compared nanofilms to nanocomposites and assessed their thermoelectric performances in the form of a figure of merit using as an example Bismuth (Bi) and p-type BismuthTelluride (Bi_2Te_3) materials. It appeared that nanofilms present higher figure of merits than the nanocomposites. However, sufficiently thin nanofilms may be more difficult to manufacture correctly than nanocomposites. Reducing the film thickness of nanocomposite materials appeared also to increase even further the figure of merit. As far as concerns the choice of nanoparticle's versus the host matrix' material, it appeared, quantitatively speaking, not straightforward. For, instance Bi nanoparticles embedded in Bi_2Te_3 showed in absolute values much higher figure of merits than Bi_2Te_3 nanoparticles embedded in Bi. Relatively, however, inclusion of Bi_2Te_3 nanoparticles into Bi showed more impact on the figure of merit than the inclusion of Bi nanoparticles into Bi_2Te_3.

The influence of particle radius and specularity on the thermoelectric properties has been investigated. A decrease in particle radius showed a better thermoelectric performance, due to more scattering of phonons and electrons. The latter effect causes a stronger decrease of the thermal conductivity than the electric one and the Seebeck coefficient (which may even increase). An increase of the specularity of the nanoparticles caused poorer thermoelectric

performances. The main reason put forward by the present model is that the smoothness of the nanoparticle surface causes less scattering (which is observed here to go against a good thermoelectric performance). Another interpretation is that higher specularities are equivalent to larger nanoparticle radii.

Generally, this work has presented that in many ways (nanofilms, nanocomposites or a combination thereof) thermoelectric properties tend to improve considerably. Via a new thermodynamic formulation, taking into account non-local effects of heat transfer by phonons and electrons (extending to electric transfer), particular phenomena have been demonstrated and explained at nanoscale.

In future work, the present model will be extended in order to calculate the efficiency of thermoelectric systems from the viewpoint of EIT. Besides the figure of merit, other phenomena can be of importance for the aforementioned efficiency, such as the mutual interaction between phonon and electron temperatures, for which it is necessary to consider a two-temperature model instead of a single one [44]. For instance, it turned out that the larger the ratio of the electron and the phonon temperature was, the higher the efficiency of a thermoelectric device was. Another possible extension is to use a nonlinear regime, since high gradients may be generated over a short length from even small differences in temperature or electric potential [45]. Finally, we can say that for future studies the present paper has investigated for the best physical conditions for the improvement of the efficiency of thermoelectric devices.

Acknowledgements

The author cordially acknowledges Prof. Georgy Lebon for valuable discussions. Financial support from BelSPo is also acknowledged.

References

[1] J.R. Baird, D.F. Fletcher, B.S. Haynes, Local condensation heat transfer rates in fine passages, Int. J. Heat Mass Tran. 46 (2003) 4453–4466.

[2] J. Lebon, D. Jou, J. Casas-Vázquez, Understanding Non-equilibrium Thermodynamics, first ed., Springer-Verlag, Heidelberg, 2008.

[3] W. He, G. Zhang, X. Zhang, J. Ji, G. Li, X. Zhao, Recent development and application of thermoelectric generator and cooler, Appl. Energy. 143 (2015) 1-25.

[4] A. Pattamatta, C.K. Madnia, Modeling heat transfer in Bi_2Te_3-Sb_2Te_3 nanostructures, Int. J. Heat Mass Tran. 52 (2009) 860–869.

[5] M.A. Ezzat, Theory of fractional order in generalized thermoelectric MHD, Appl. Math. Model. 35 (2011) 4965-4978.

[6] J.E. Cornett, O. Rabin, Thermoelectric figure of merit calculations for semiconducting nanowires, Appl. Phys. Lett. 98 (2011) 82184.

[7] A. Sellitto, V.A. Cimmelli, D. Jou, Thermoelectric effects and size dependency of the figure-of-merit in cylindrical nanowires, Int. J. Heat Mass Tran. 57 (2013) 109–116.

[8] D.C. Moreira, L.A. Sphaier, J.M.L. Reis, L.C.S. Nunes, Experimental Investigation of Heat Conduction in Polyester–Al_2O_3 and Polyester–CuO Nanocomposites, Exp. Therm. Fluid Sci. 35 (2011), 1458-1462.

[9] J. Chen, S.L. Li, Z.L. Tao, L.Z. Zhang, Reversible Hydrogen and Lithium Storage of MoS_2 Nanotubes, Int. J. Nanosci. 1 (2002) 295-302.

[10] T. Sun, M.K. Samani, N. Khosravian, K.M. Ang, Q. Yan, B.K. Tay, H.H. Hng, Enhanced thermoelectric properties of n-type $Bi_2Te_{2.7}Se_{0.3}$ thin films through the introduction of Pt nano inclusions by pulsed laser deposition, Nano Energy 8 (2014) 223–230.

[11] W. Liu, X. Yan, G. Chen, Z. Ren, Recent advances in thermoelectric nanocomposites, Nano Energy 1 (2012) 42–56.

[12] H. Alama, S. Ramakrishna, A review on the enhancement of figure of merit from bulk to nano-thermoelectric materials, Nano Energy 2 (2013) 190–212.
[13] M.E. Lynch, D. Ding, W.M. Harris, J.J. Lombardo, G.J. Nelson, W.K.S. Chiu, M. Liu, Flexible multiphysics simulation of porous electrodes: Conformal to 3D reconstructed microstructures, Nano Energy 2 (2013) 105–115.
[14] K.K. Choudhary, D. Prasad, K. Jayakumar, D. Varshney, Effect of Embedding Nanoparticles on Thermal Conductivity of Crystalline Semiconductors: Phonon Scattering Mechanism, Int. J. Nanosci. 8 (2009) 551-556.
[15] D. Jou, J. Casas-Vazquez, G. Lebon, Extended Irreversible Thermodynamics, fourth ed., Springer-Verlag, Berlin, 2010.
[16] G. Lebon, H. Machrafi, M. Grmela, Ch. Dubois, An Extended Thermodynamic Model of Transient Heat Conduction at Sub-Continuum Scales, P. Roy. Soc. A-Math. Phy. 467 (2011) 3241-3256.
[17] C. Cattaneo, Sulla conduzione del calore, Atti del Seminario Matematico e Fisico delle Università di Modena 3 (1948) 83-101.
[18] D. Jou, J. Cásas-Vazquez, G. Lebon, Extended irreversible thermodynamics of heat transport. A brief introduction, Proc. Eston. Ac. Sci., 57 (2008) 118-126.
[19] W. Dreyer, H. Struchtrup, Heat Pulse Experiments Revisited, Continuum. Mech. Therm. 3 (2003) 3-50.
[20] S. Hess, On Nonlocal Constitutive Relations, Continued Fraction Expansion for the Wave Vector Dependent Diffusion coefficient, Z. Naturforsch. 32a (1977) 678-684.
[21] N. Satyala, A.T. Rad, Z. Zamanipour, P. Norouzzadeh, J.S. Krasinski, L. Tayebi, D. Vashaee, Reduction of thermal conductivity of bulk nanostructured bismuth telluride composites embedded with silicon nano-inclusions, J. Appl. Phys. 115 (2014) 044304.
[22] N. Satyala, A.T. Rad, Z. Zamanipour, P. Norouzzadeh, J.S. Krasinski, L. Tayebi, D. Vashaee, Influence of germanium nano-inclusions on the thermoelectric power factor of bulk bismuth telluride alloy, J. Appl. Phys. 115 (2014) 204308.
[23] N.W. Gothard, The effects of nanoparticle inclusions upon the microstructure and thermoelectric transport properties of Bismuth Telluride-based composites, PhD dissertation, Clemson University (2008) pp.118-119.
[24] E. Cimpoiasu, E. Stern, G. Cheng, R. Munden, A. Sanders, M. A. Reed, Electron mobility study of hot-wall CVD GaN and InN nanowires, Braz. J. Phys. 36(3b) (2006) 824-827.
[25] H. Foell, Semiconductors I, Chapter 2, *lecture notes*, University of Kiel (2014).
[26] A. Minnich G. Chen, Modified Effective Medium Formulation for the Thermal Conductivity of Nanocomposites, Appl. Phys. Lett. 91 (2007) 073105.
[27] C.W. Nan, R. Birringer, D.R. Clarke, H. Gleiter, Effective Thermal Conductivity of Particulate Composites with Interfacial Thermal Resistance, J. Appl. Phys. 81 (1997) 6692-6699.
[28] J. Ordonez-Miranda, R. Yang, J.J. Alvarado-Gil, On the Thermal Conductivity of Particulate Nanocomposites, Appl. Phys. Lett. 98 (2011) 233111.
[29] J.C. Maxwell, Treatise on Electricity and Magnetism, second ed., Clarendon, Oxford, 1881.
[30] D. Bruggeman, Berechnung verschiedener physikalischer Konstanten von heterogenen Substanzen, Anal. Phys. 24 (1935) 636-664.
[31] G. Chen, Thermal conductivity and Ballistic-phonon Transport in the cross-plane Direction of Superlattices, Phys. Rev. B 57 (1998) 14958-14973.
[32] H.J. Goldsmid, Bismuth -- The Thermoelectric Material of the Future?, 25th International Conference on Thermoelectrics (2006), pp. 5-10.
[33] H.J. Goldsmid, Bismuth Telluride and its alloys as materials for thermoelectric generation, Materials, 7 (2014) 2577-2592.

[34] S. Cho, Y. Kim, A.J. Freeman, G.K.L. Wong, J.B. Ketterson, L.J. Olafsen, I. Vurgaftman, J.R. Meyer, C.A. Hoffman, Large magnetoresistance in postannealed Bi thin films, Appl. Phys. Lett. 79 (2001) 3651.
[35] J.S. Jin, Prediction of phonon and electron contributions to thermal conduction in doped silicon film, J. Mech. Sci. Technol. 28 (2014) 2287-2292.
[36] O. Madelung, U. Rössler, M. Schulz, Bismuth (Bi) effective masses – Non-Tetrahedrally Bonded Elements and Binary Compounds I, pp. 1-11, Springer, Berlin, 1998.
[37] E.G. Gamaly, A.V. Rode, Is the ultra-fast transformation of bismuth non-thermal?, arXiv:0910.2150 [physics.optics], (2009).
[38] E.G. Gamaly, A.V. Rode, Ultrafast electronic relaxation in superheated bismuth, New J. Phys. 15 (2013) 013035.
[39] J.L. Pélissier, N. Wetta, A model-potential approach for bismuth (I). Densification and melting curve calculation, Physica A 289 (2001) 459-478.
[40] J.P. Issi, A. Luyckx, Size effect in the thermopower of Bismuth, Phys. Lett., 23 (1966) 13-14.
[41] D. Jou, A. Sellitto, V.A. Cimmelli, Multi-temperature mixture of phonons and electrons and nonlocal thermoelectric transport in thin layers, Int. J. Heat Mass Tran. 71 (2014) 459–468.
[42] O. Madelung, U. Rössler, M. Schulz, Bismuth Telluride (Bi) effective masses – Non-Tetrahedrally Bonded Elements and Binary Compounds I, pp. 1-4, Springer, Berlin, 1998.
[43] C.B. Satterthwaete, R.W. Ure jr., Electrical and thermal properties of Bi_2Te_3, Phys. Rev. 108 (1957) 1164-1170.
[44] A. Sellitto, V. A. Cimmelli, D. Jou, Influence of electron and phonon temperature on the efficiency of thermoelectric conversion, Int. J. Heat Mass Transf., 80 (2015) 344-352.
[45] V. A. Cimmelli, A. Sellitto, D. Jou, A nonlinear thermodynamic model for a breakdown of the Onsager symmetry and the efficiency of thermoelectric conversion in nanowires, Proc. R. Soc. A, 470 (2014) 20140265 (13 pages).